NAVAL AIR WARFARE CENTER AIRCRAFT DIVISION

PATUXENT RIVER, MARYLAND

TEST PLAN / TEST RESULTS (PRELIMINARY DRAFT)

High Energy Electromagnetic Field Generation
Coin Cell Capacitor Spin Test

NAVAIR 4.4.6
Propulsion & Power
Test Methods & Facilities Department

1 October 2018

Prepared by:
(b) (6)
AIR 4.4.6.4

Table of Contents

BACKGROUND

1. The Rotor Spin Facility (RSF) in the Propulsion System Evaluation Facility (PSEF) has been requested to perform a spin test on a charged disk test article to evaluate the concept of High Energy Electromagnetic Field Generation (HEEMFG). Salvatore Pais Ph.D. is the Principal Investigator (PI) for this testing which is sponsored by the Naval Innovative Science & Engineering (NISE) program under the category of Basic & Applied Research (BAR). The concept of HEEMFG and its governing physics was proposed by Salvatore Pais Ph.D., AIR 4.3.5.1, in a paper titled "The high energy electromagnetic field generator" published in the International Journal of Space Science and Engineering, Vol.3, No. 4, 2015 pp.312-317.; this article is included in Appendix A.

2. The HEEMFG effect is described as very high energy electromagnetic field intensities resulting from accelerated spin of a highly charged (excess electrons) disk, in a vacuum, at high speeds, with acceleration transients and vibration. When put into practice, the HEEMFG effect could be used toward the design of advanced high energy density/ high power propulsion systems.

3. Initial efforts on this program focused on the design of a charged disk test article configured as a parallel plate capacitor capable of rotational speeds approaching 100,000 rpm but without a method for inducing disk vibration. A design using a ceramic dielectric sandwiched between two 3.25" diameter metal disks, incorporating a button cell battery to maintain the charge, was about 80% complete and test spins on the button cell battery (.189" diameter) proved survivability at speed was acceptable (25 minutes at 100,000 rpm); recently however, the parallel plate capacitor design effort was suspended in preference to using a commercial off-the-shelf (COTS) coin cell capacitor (.276" diameter) with orders of magnitude greater charge carrying capability and potential for high speed operation due to its similarity in size and construction to the high speed capable button cell battery.

4. For quantitative detection of the HEEMFG effect, COTS sensors were considered to measure the frequency and calibrated amplitude of emitted electro-magnetic (EM) flux of the spinning charged disk; where 'flux' is power per unit area. COTS EM flux sensors operate over very narrow frequency bands and are directional in nature. Multiple COTS sensor systems would be needed to cover the wide 3 Hz to 3.2 GHz frequency band of interest. To reduce complexity and cost of the measurement, the team decided to design an EM flux detector with a single sensor covering the entire bandwidth of interest but with an un-calibrated relative amplitude output for qualitative only indication of the HEEMFG effect.

5. The current spin test effort is now focused on using a small COTS coin cell super capacitor to serve as the charged disk test article and an in-house designed and fabricated EM flux detector to measure the presence and relative strength of the emitted EM flux (HEEMFG effect).

6. The theoretical prediction by the PI for maximum EM flux intensity for a coin cell capacitor in non-accelerated spin at 4775 rpm (500 rad/s) in extreme proximity to the test article (~ 10^{-5} meters) is on the order of 10^{21} watts per meter squared; **this is a maximum theoretical value without any experimental validation.**

PURPOSE AND OBJECTIVE OF TEST

7. The purpose of this test is to evaluate the presence of the HEEMFG effect resulting from spinning a charged disk, in the form of a coin cell capacitor, to high speeds with rapid acceleration transients.

SCOPE OF TEST

8. The scope of this test program includes a) in-house development of instrumentation to qualitatively detect the HEEMFG effect; b) design of a capacitor test circuit, c) design of adaptive spin tooling; and d) spin testing of a coin cell capacitor to evaluate the HEEMFG effect.

9. Detection of the HEEMFG effect will be accomplished with an experimental EM flux detection circuit and a single receiving antenna surrounding the capacitor test article to receive radio frequency (RF) waves presumed to be generated when the HEEMFG effect occurs. The EM flux detector and antenna will be developed in a bench test environment and require multiple design iterations. Detection of low power level (1 milliwatt) RF waves over a 3 Hz to 3.2 GHz bandwidth is the goal. The EM flux detector circuit will convert the antenna signal to an EM flux relative amplitude (un-calibrated) for monitoring and recording on the APEX high speed data system; this will serve as a qualitative indication of the HEEMFG effect.

10. A constant current capacitor load test circuit will be designed/fabricated to evaluate the state of charge of the capacitor before and after spin test runs.

11. Tooling will be designed to adapt the capacitor to the facility drive hardware so that the capacitor spins about its geometric center.

12. The spin test to evaluate the HEEMFG effect will run a coin cell capacitor to the speed versus time mission profiles supplied by the PI, shown in figure 1 below; there are two profiles, one with low acceleration rates, up to 2000 rpm/s and one with high acceleration rates, up to 5000 rpm/s. If necessary, the mission profile RPM values will be adjusted downward to match the capacitor's maximum speed capability once this is determined from test runs.

Low Acceration			High Acceleration		
Elapsed time (sec)	RPM (Mission Low Accel.)	Acceleration (rpm/s)	Elapsed time (sec)	RPM (Mission High Accel.)	Acceleration (rpm/s)
0	0		0	0	
20	5,000	250	20	5,000	250
40	10,000	250	30	7,500	250
60	20,000	500	60	30,000	750
80	40,000	1,000	100	15,000	-375
100	80,000	2,000	120	55,000	2,000
120	100,000	1,000	150	80,000	833
140	100,000	0	200	60,000	-400
160	80,000	-1,000	220	100,000	2,000
180	40,000	-2,000	240	7,500	-4,625
200	20,000	-1,000	300	90,000	1,375
220	10,000	-500	320	5,000	-4,250
240	5,000	-250	340	100,000	4,750
260	0	-250	360	0	-5,000

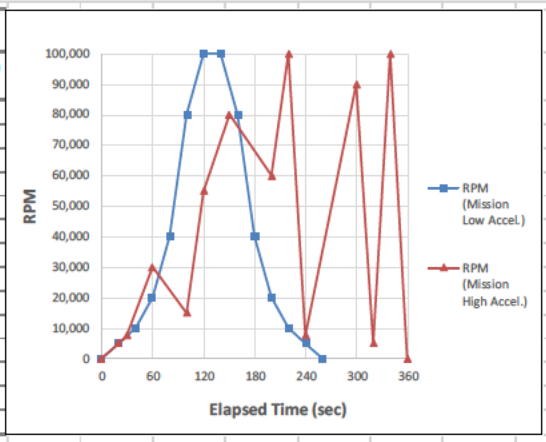

Figure 1 – Capacitor Mission Cycle Profiles

13. The capacitor mission profiles will be run under the following test conditions: capacitor spinning in the clockwise direction (viewed from above), capacitor fully charged up to 5.6 coulombs, spin chamber at vacuum level of .5 torr or less and ambient temperature, and capacitor radial displacement levels up to 25 mils Peak-to-Peak (PtP) as sub-synchronous (~ 700 Hz +/-) whirl vibration. Test conditions are summarized in table 1 below.

Table 1 – HEEMFG Spin Test Conditions

Speed Range	5000 rpm to 100,000 rpm (max speed contingent on capacitor performance)
Over-speed Limit	102,000 rpm
Test Article Temperature	Ambient
Capacitor Charge	Up to 5.6 coulombs
Rotor Speed Profile	See Figure 1
Chamber Vacuum	<500 mTorr (Best Achievable)
Test Article Vibration Limits	30 mils-PtP @ 0 rpm to 100,000 rpm
Direction of Rotation	Clockwise from above

14. The spin test will include a series of test runs working up to the planned mission profile test runs. The test run matrix is given in table 2. Individual test runs may need to be run multiple times to establish repeatability.

Table 2 – Test Runs Matrix

Test	Test Name	Test Article	Speed Profile	Capacitor Charge (coulombs)	Antenna Installed	Proximity Probe Power	Chamber Vacuum	Inspection/ Capacitor Load Test
Stage 1: EM Flux Detector/Antenna Performance Evaluation in Spin Chamber								
1	EM flux detector eval. - prox. probe off	dummy	static	n/a	yes	off	< 5 torr	no
2	EM flux detector eval. - prox. probe on	dummy	static	n/a	yes	on	< 5 torr	no
Stage 2: Air Motor Funtional Checkout and Speed Controller Tuning - No Antenna								
3	Air motor checkout - stair step	none (threaded spindle only)	0 - 100 krpm in 10krpm steps at 5000 rpm/s	n/a	none	on	< 5 torr	no
4	Air motor checkout - slow sweep	none (threaded spindle only)	500 rpm/s: 0 to 100 krpm to 0	n/a	none	on	< 5 torr	no
5	Air motor checkout - mission low	none (threaded spindle only)	mission low	n/a	none	on	< 5 torr	no
6	Air motor checkout - mission high	none (threaded spindle only)	mission high	n/a	none	on	< 5 torr	no
Stage 3: Trial Running of Test Vehicle with Dummy Capacitor to Determine Max Speed Capability - Blank Antenna Mandrel Installed								
7	Test Vehicle checkout - stair step	dummy	0 - 100 krpm at 5000 rpm/s beginning at 50 krpm, in 10 krpm increments, up or down as req'd, with 6 minute of dwell each incement	n/a	blank mandrel	on	< 5 torr	yes, after each increment
8	Test Vehicle checkout - max. accel./decel	dummy	max. accel/decel rate snaps to/from100krpm or max speed from above	n/a	blank mandrel	on	< 5 torr	yes
Stage 4: Trial Running of Dummy Capacitor Test Vehicle to Establish EM Flux Baseline Noise Level - Antenna Installed								
9	Baseline - static	dummy	static	n/a	yes	off	< 5 torr	no
10	Baseline - stair step	dummy	0 - test vehicle max rpm at 5000 rpm/s beginning at 50 krpm, in 10 krpm increments, upr or down as required, with 6 minute of dwell each incement	n/a	yes	off	< 5 torr	multiple
11	Baseline - slow sweep	dummy	500 rpm/s: 0 - test vehicle max - 0	n/a	yes	off	< 5 torr	no
12	Baseline - mission low	dummy	mission - low accel (limit to test vehicle max speed)	n/a	yes	off	< 5 torr	no
13	Baseline - mission high	dummy	mission - high accel (limit to test vehicle max speed)	n/a	yes	off	< 5 torr	no
Stage 5: Spin Test of Charged Capacitor to Evaluate HEEMFG Effect - Antenna Installed								
14	Capacitor -static	capacitor	static	5.6	yes	off	< 5 torr	no
15	Capacitor - stair step	capacitor	0 - test vehicle max rpm at 5000 rpm/s beginning at 50 krpm, in 10 krpm increments, upr or down as required, with 6 minute of dwell each incement	5.6	yes	off	< 5 torr	multiple
16	Capacitor - slow sweep	capacitor	500 rpm/s: 0 - capacitor max - 0	5.6	yes	off	< 5 torr	yes
16	Capacitor - mission low	capacitor	mision - low accel (limit to capacitor max speed)	5.6	yes	off	< 5 torr	yes
17	Capacitor - mission high	capacitor	mision -high accel (limit to capacitor max speed)	5.6	yes	off	< 5 torr	yes
18	Capacitor - mission low max. accel.	capacitor	misson high with max accel/decel rates snaps at speed set points (limit to capacitor max speed)	5.6	yes	off	< 5 torr	yes
19	Capacitor - mission high max. accel.	capacitor	misson low wi h max accel/decel rates snaps at speed set points (limit to capacitor max speed)	5.6	yes	off	< 5 torr	yes

TEST SCHEDULE

15. The schedule is as follows:

Task Description	Timeframe
EM flux Detection Instrumentation Develop/Design/Fabricate/Evaluate	October 2017 – August 2018
Coin Cell Capacitor Adaptive Tooling Design/Fabricate:	May – August 2018
Test Setup/Calibrations in Chamber #4	February – August 2018
Conduct Coin Cell Capacitor Spin Test	**September 2018**
Report Results	September 2018

TEST TEAM

16. Core team members are listed in table 3 below.

Table 3 - HEEMFG Spin Test Team

Personnel	Code	Position	Phone Number
(b) (6)	4.3.5.1	NISE Principal Investigator/Program Engineer	(b) (6)
(b) (6)	4.4.5.1	NISE Program Engineer	(b) (6)
(b) (6)	4.4.6.4	Test & Evaluation Engineer	(b) (6)
(b) (6)	4.4.6.4	Test & Evaluation Engineer	(b) (6)
(b) (6)	4.4.6.4	Test & Evaluation Engineer	(b) (6)
(b) (6)	4.4.6.3	Engineering Test Technician	(b) (6)
(b) (6)	4.4.6.3	Test Mechanic	(b) (6)
(b) (6)	4.4.6.5	Instrumentation	(b) (6)
(b) (6)	4.4.6.5	Instrumentation	(b) (6)
(b) (6)	4.4.6.5	Instrumentation	(b) (6)
(b) (6)	4.4.6.5	Instrumentation	(b) (6)

DESCRIPTION OF TEST FACILITY

17. The NAVAIR Rotor Spin Facility (RSF) is located within the Propulsion Systems Evaluation Facility (PSEF), building 2360, Patuxent River, MD. The RSF operates four above-ground vacuum spin chambers with inner diameters ranging from 24" to 106" designed to spin turbomachinery components up to design speeds to evaluate the structural and material aspects of rotating gas turbine engine components under simulated engine conditions. Spin tests are typically conducted in a vacuum to reduce the power required to drive the test article and to reduce the explosive hazards when testing at high temperatures. Spin testing always carries the risk of catastrophic failure of the component under test, so the spin chambers are designed to safely contain the release of high energy fragments; the safety containment features include thick annular steel rings for radial containment and a spin lid retention system for axial containment.

18. Barbour Stockwell, Inc. (BSI) vertical drive shaft air motors (or drive turbine) are used to drive the test rotors. The RSF has a range of air motors sizes, from 1.5” to 14”, to handle test articles up to 4000 lbs. and speeds up to 150,000 rpm and has the capability to conduct heated tests up to 2000 degrees Fahrenheit. The air motor and test rotor are assembled to a removable spin chamber lid in a separate build up shop and then transported by overhead crane to the spin chamber. Spin chambers are operated from a remotely located control room with independent controls and data acquisition for each chamber. Reinforced concrete walls separate the spin chamber from the buildup shop and control room for personnel safety. The spin test controls are set up to allow unmanned 24/7 automated cycling of test rotors and automatic shutdown of the test when test rotor or air motor health parameters exceed preset limits.

19. The RSF has three 2600 cfm compressors supplying compressed air to the air motors that drive the tests. Each chamber has a BSI model TC-4 automated speed controller that controls the supply of air to the air motor for cyclic or dwell control of test rotor speed. Each chamber has its own vacuum pump to evacuate the chamber with testing performed at best achievable vacuum below 1 torr, typically around 0.5 torr. Each chamber has a Pacific model 6000 data acquisition system for recording test rotor and facility parameter data, display of data for real-time monitoring, signal conditioning for the majority of parameters, and safety shutdown capability.

20. RSF has one APEX high speed data system capable of recording signals at 200 kHz sample rate with software for monitoring, recording and playback of the resulting large data files. ***The APEX system will be used to record the EM flux Detector output signal for primary indication of the HEEMFG Effect.***

DESCRIPTION OF TEST ARTICLE

21. The article under test is a coin cell style polarized energy storage capacitor with high capacity and energy density, Vishay order code MAL219691131E3. It is low cost at $5 each. It was chosen for its high charge capacity, its ability to survive spin chamber vacuum conditions, and its small diameter to minimize the centrifugal loads developed at high rotational speed. It is 0.276” diameter by .098” tall overall and weighs .28 grams.

22. The capacitance is 4 Farads +0/-20% with a rated voltage of 1.4 volts and designed for maximum discharge current of 25 milliamps. At the rated 1.4 volts, the maximum charge capacity is 5.6 coulombs

(charge = volts x capacitance); dividing this charge by the nominal cross-section area gives a charge density for the negative (-) surface of 145,500 coulombs per m^2.

23. As shown in the representative cutaway view in figure 2, the capacitor is constructed with a two-piece metal outer shell and an internal gasket sealing the electrode/non-hazardous electrolyte. The capacitor comes from the factory pre-charged, with a plastic film on the OD and solder tabs for horizontal installation on a circuit board – the plastic and solder tabs will be removed for this test.

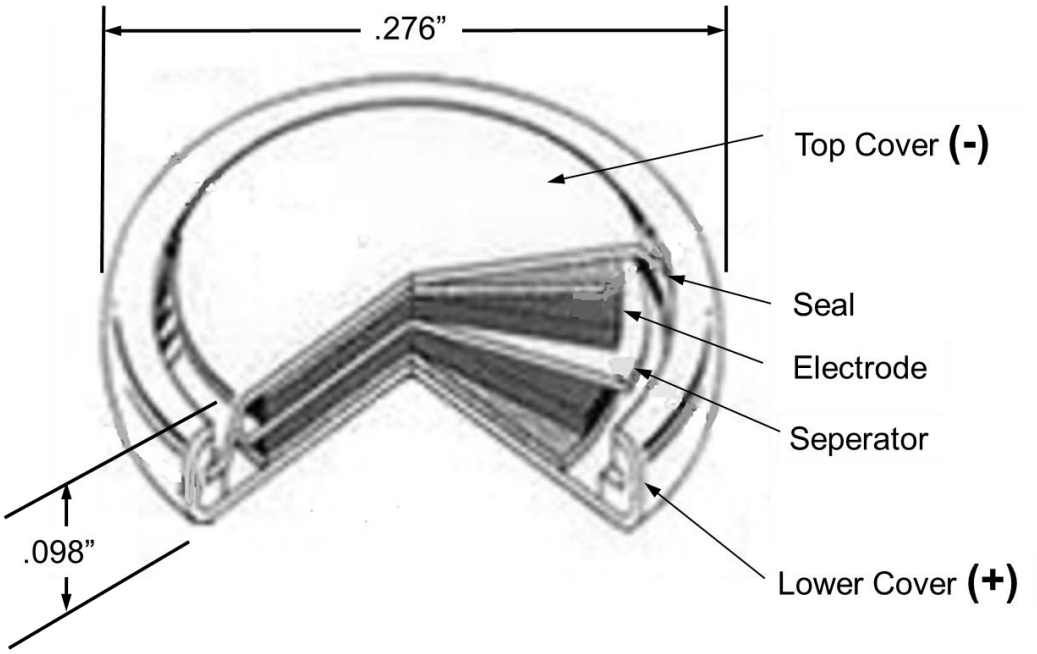

Figure 2. Coin Cell Capacitor – Representative Cutaway

24. Short circuiting of the capacitor terminals is permitted, but not permanently. Short circuiting of charged cells may heat up the cells. Polarity must be observed when charging the capacitor – reverse polarity charging will cause the capacitor to burst energetically. Exceeding the rated voltage will damage the capacitor. Selected pages from the Vishay specification document are in included in Appendix A for reference.

DESCRIPTION OF INSTALLATION AND TEST EQUIPMENT

Test Setup

25. The test will be performed in RSF spin chamber #4 located in PSEF room 72. Chamber #4 is the smallest of the four spin chambers accommodating rotors up to 24". The chamber overall nominal dimensions are 58.5" OD x 41" tall.

26. The test setup is shown in figure 3 below. It consists of an air motor, spin lid, capacitor test vehicle and vacuum chamber with steel containment (not shown). A BSI model 7890 air motor will drive the test and is powered by facility compressed air at 70 psig. The air motor's 5/16" diameter vertical drive spindle extends down through the spin lid. For this test, external threads have been added to the end of the spindle. A plastic capacitor holder threads onto the spindle to hold the capacitor concentric with the spindle's axis of rotation. The capacitor's negative (-) face points down and the positive (+) face is electrically isolated from the spindle by a .06" thick nylon spacer.

27. The air motor's rotor is supported in two ceramic bearings (electrically non-conductive) and held in place axially with a rotor locknut. Rotational speed is measured using the 6 pulse per revolution output of a hall-effect sensor reading the 6 toothed rotor locknut. The spindle's top end is connected to the rotor and constrained in the radial direction; the bottom end of the spindle is free to move in the radial direction. One of two installed proximity probes will be used to monitor spindle's radial displacement (wobble). An aluminum probe mount designed specifically for this test positions the probes about 1" axially above the test article. During tests where the HEEMFG effect will be enabled, the proximity probes will be powered off and lead ends stowed in a metal box to prevent electromagnetic interference (EMI).

28. Detection of EM flux will be accomplished with a receiving antenna surrounding the test article and mounted to the proximity probe mount; the radial clearance between the antenna ID and capacitor holder OD is .06". The antenna's output is connected to an EM flux detector circuit mounted in a metal box on the spin lid, outside the spin chamber; the box is electrically grounded to the spin lid. The output of the EM flux Detector connects to an APEX high speed data system located in the control room via a 100+ feet of EMI shielded signal cable. The APEX system will be used to monitor and record the output signal for indication of the HEEMFG Effect.

29. The all metal spin chamber entirely encloses the test article and acts as a faraday cage to shield the test setup from unwanted external electromagnetic interference (EMI or noise) that could interfere with the EM flux measurement and/or cause a false positive indication.

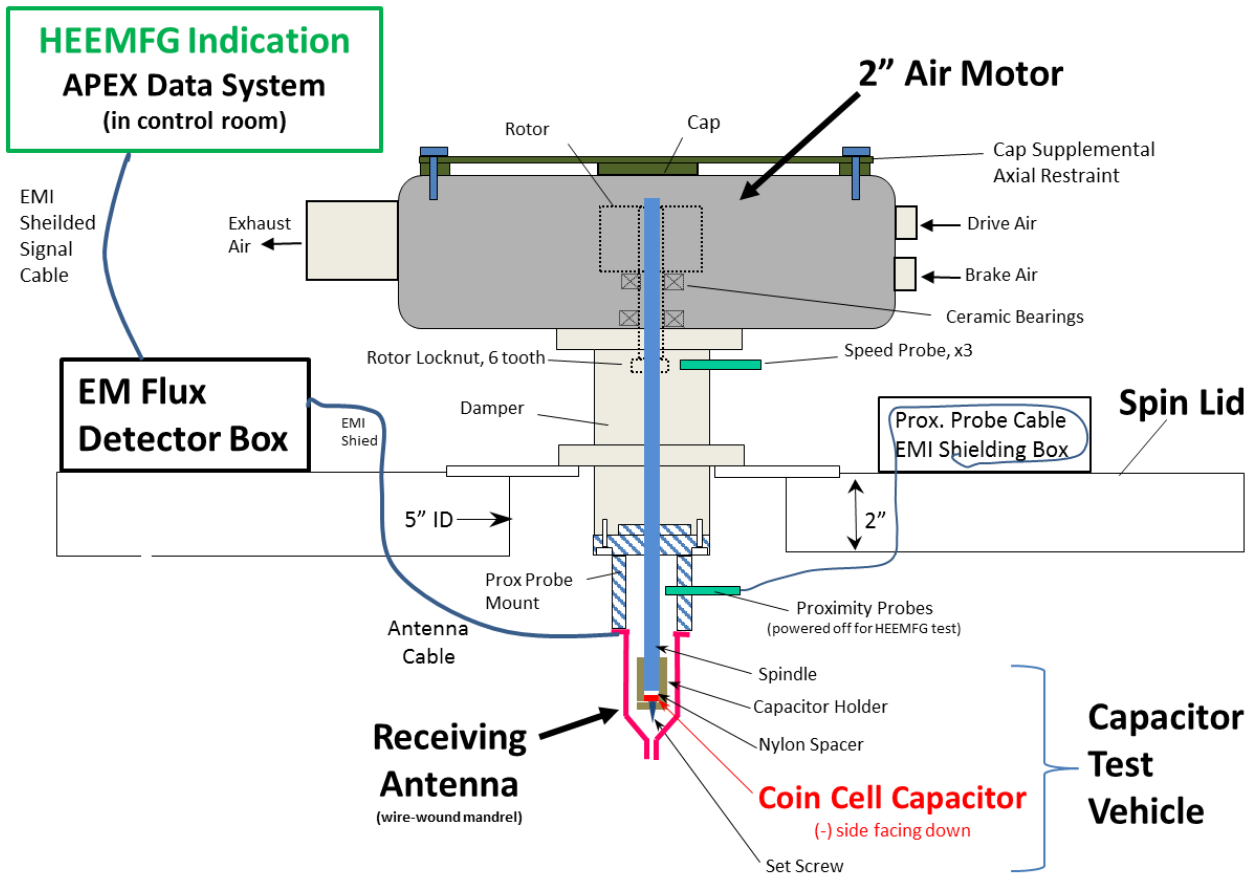

Figure 3. Spin Test Setup

Capacitor Test Vehicle Description

30. A cross-section view of the rotating *Capacitor Test Vehicle* is given in figure 4 below. The test vehicle consists of the capacitor and the adaptive tooling mounting it to and electrically isolating from the spindle. The adaptive tooling consists of a spindle, capacitor holder, nylon spacer, and set screw. Overall dimensions are 11.3" tall x .433 diameter and overall assembly weight is 105 grams. Test vehicle component and assembly details are given below.

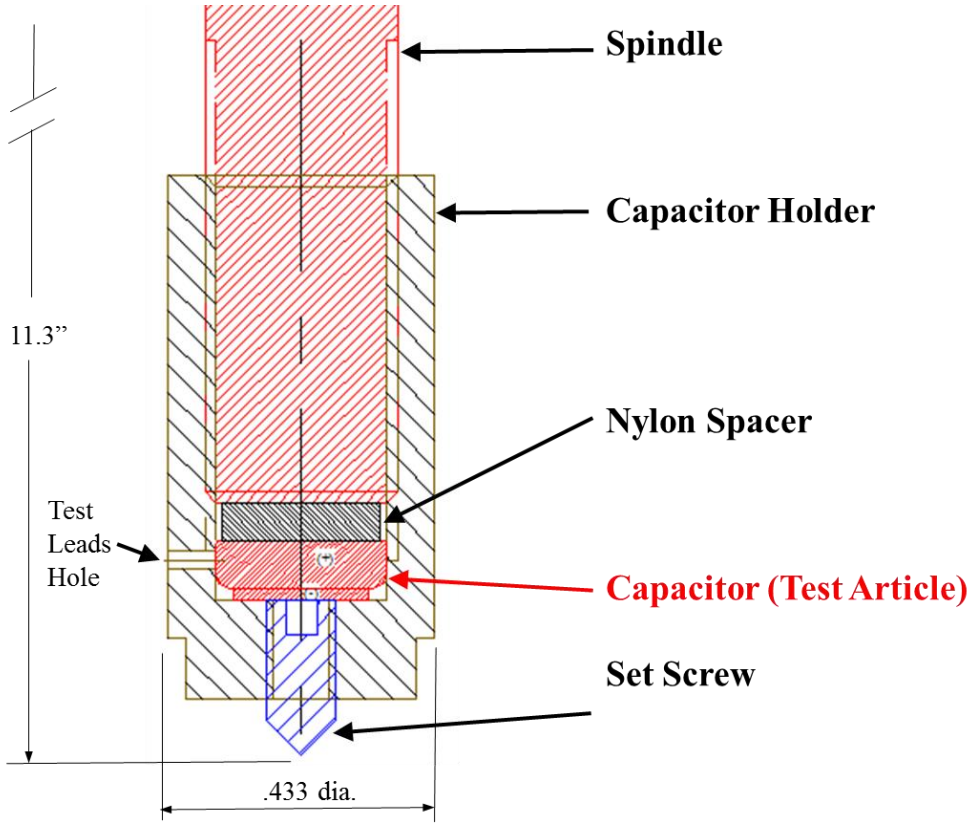

Figure 4 – Capacitor Test Vehicle

31. The *Spindle* is a BSI model 2529RH solid steel vertical drive spindle (5/16” dia. X 11”) modified to add external threads, 5/16”-24 x .75”, to the non-driven end and length shortened by .4”. The driven-end has the standard ¼” square drive and ¼”-28 thread feature for connection to the air motor’s turbine rotor. Weight is 102 grams.

32. The *Capacitor Holder* threads onto the non-driven end of the spindle to hold the capacitor captive and clamp it against the end of the spindle. It is made from Torlon 4203 high strength thermoplastic which is non-conductive and transparent to RF energy. A .035” radial hole and #4-40 threaded axial hole provide access for test leads. Threadlocker (Loctite 425) is used to prevent loosening. Weight is 1.75 grams.

33. A *Nylon Spacer* is used to electrically isolate the capacitor from the spindle. The spacer is punched from .06” thick nylon sheet using a 17/64” diameter hole punch for a close tolerance fit with the capacitor holder ID. Weight is .12 grams.

34. The *Capacitor (Test Article)* is oriented with negative (-) plate facing down and close tolerance fit with the Capacitor Holder ID. Weight is .28 grams.

35. A stainless steel *Set Screw,* in electrical contact with the capacitor, extends the capacitor's negative (-) charge to a point which may improve the transmission of HEEMFG effect energy to the receiving antenna. The set screw is a #4-40 x .25" cone point style. Threadlocker (Loctite 425) is used to prevent loosening. Weight is .17 grams.

Test Equipment

36. The test equipment required to run the test is described below:

37. *Spin Chamber #4* is a nominal 59" OD x 41" tall overall steel vacuum chamber located in PSEF test room #72. The pressure wall is 1" thick. The metal vacuum chamber acts a faraday cage for this experiment to keep EMI noise out of measurement and any radiation generated by the HEEMFG effect inside the chamber.

38. *Spin Chamber Lid:* The air motor is mounted to the top side of the spin chamber lid and has a 5" diameter center hole for passage of the vertical drive spindle. An integral hydraulic lift makes spin lid removal and access to the test vehicle quick and convenient as the overhead crane is not required. The spin lid and air motor assembly can be raised, lowered, and swiveled 180° to facilitate test article installation and inspections.

39. *Safety Radial Containment:* Permanently installed 4 inch radial thickness lead bricks inside of a 4 inch radial thickness steel ring provide containment of high speed rotor fragments in the radial direction should the test rotor fail catastrophically. It should be noted that the coin cell capacitor test vehicle axial location is above this containment; however, it is in the plane of the spin chamber's 4 inch radial thickness top flange (2" axial height).

40. *2" Air Motor with supplemental cap restraint:* Barbour Stockwell Inc. (BSI) model 7890 air motor with a standard damper section is used to drive the test article via a 5/16"" OD x 11.7" long drive spindle. Air motor peak power output is about 11 KW (90psig air supply*).* The air motor's turbine rotor is supported in two ceramic bearings and transmits torque to the spindle via a ¼" square drive. A ¼"-28 locknut secures the spindle axially to the rotor. The damper section has a squeeze film style damper, with spring loaded oil cups, to reduce lateral vibrations in the spindle. Facility owns 2. A ¼" thick steel bar is bolted to the top of the turbine to provide supplemental axial restraint for the air motor aluminum cap. This is risk mitigation to ensure the air motor's rotor stays contained within the air motor during an overspeed event separating it from the bearing support shaft.

41. *Air Compressor:* Supplies compressed air to power the 2" air motor that drives the test vehicle. RSF has three centrifugal compressors available for spin testing, each can generate 2600 SCFM @ up to 140 psig. About 10% capacity of one compressor is sufficient for this test.

42. *Drive System Speed Control:* Air motor speed control is handled by the Barbour Stockwell TC4 cycle controller in conjunction with the SPIN IV software. Using the speed signal (6 per revolution) as feedback, the TC4 controls the flow of compressed air supplied to the drive and brake portions of the 2" air motor to

accelerate and decelerate the test vehicle under automatic control to run the programmed mission cycle profile specified for the test.

43. *Air Supply Valves:* Compressed air from the facility 3" supply manifold is regulated through a 2" proportional valve and supplied to the air motor; it is distributed via 2" plumbing through two 3" fast acting butterfly valves that provide on/off control of the air flow through 1" hoses connected to the brake and drive portions of the air motor.

44. *Lubrication System:* An external oil lubrication cart is used to service the bearings and damper section of the drive turbine throughout testing. SHC-824 oil is used for the test system. In the event of a power outage, oil pumps are powered by a backup generator and/or compressed air driven motor.

45. *Vacuum System:* The test cell housing spin chamber #4 is equipped with one Kinney model KT300 vacuum pump with KMBD850 vacuum booster to evacuate the chamber. It is used to reduce the test cell vacuum to below 1 Torr or better.

INSTRUMENTATION AND DATA ACQUISITION

46. Instrumentation and data acquisition systems required to run the test are described below:

47. *Speed Measurement:* Rotational speed is measured using the 6 pulse per revolution output of a hall-effect sensor reading the air motor's 6 toothed rotor locknut. There are three sensors installed in 1/4"-40 threaded ports in the damper section of the air motor; they are spaced at 0° (OEM port), 120°, and 220°. The sensor gap should be set to .035 to .040. The sensors are SPECTEC model 0165A-73102 (or the 12" leadwire version 0165A-03C or alternatively a Barbour Stockwell model T-C-3-45); SPECTEC sensor is NPN w/internal 3k Ohm pull-up, normally high.

48. *Spindle Radial Displacement:* Radial displacement (wobble) of the drive spindle will be monitored using one of two eddy-current *proximity probes* mounted 90° apart and axially positioned about 1" axially above the end of the spindle. The sensor is an SKF model CMSS65 probe with ¼"-28 x 1.2" threaded barrel, a 5 meter system length, a model CMSS665 driver, and sensitivity of 200 mv/mil. The sensor will be gapped at .05" from the spindle. The raw output signal is converted to a 4 to 20 milliamp analog signal proportional to peak-to-peak displacement using a vibration transmitter, STI Vibration Monitoring Inc., model CMCP540-200-MOD3X; this transmitter is a special version designed to provide a ripple free output above 500 rpm.

49. For this test configuration, only one proximity probe can be powered on at any given time; otherwise, the probes will interfere with each other because the mounting arrangement does not meet the 1" minimum probe tip spacing requirement. **Both probes will be powered off during EM flux measurement runs to prevent electro-magnetic interference (EMI)**; **additionally, the probe lead ends outside the spin chamber will be disconnected and stored coiled up inside an EMI shielding box mounted on the spin lid**. This displacement signal is used to trigger an automatic test shutdown when a threshold value is exceeded.

50. *Chamber temperature* is measured by a metal sheathed thermocouple about 1" below the lid. It is installed with metal to metal contact with the chamber through a penetration in the spin lid. The sheath must be in metal contact with the spin lid to avoid potential EMI noise in the EM flux measurement.

51. A *Distributed Control System (DCS)* will provide signal conditioning, display, and safety shutdowns for speed and shaft radial displacement parameters. It will provide speed signal updates at 10 times per second and provide the median value of the three measured speed signals for display and recording by other data systems.

52. A *PACIFIC Data Acquisition and Signal Conditioning System* provides signal conditioning for most sensors, recording of data, and safety shutdowns (excluding speed and radial shaft displacement which are being handled by a DCS). The system's single scan mode will be used to capture data parameters at a rate of 10 samples/sec per channel into an Excel readable text file. The data system will be set to record during all test activities when the rotor is spinning. A single text file will contain all the runs for a single test day; the test day date will be embedded in the filename for easy identification. The data files will be archived to the RSF share drive on a daily basis. Note that the sample rate on this system is not fast enough to register transient signals from the EM flux detector.

53. An *ASTRO-MED Strip Chart Recorder* provides a permanent paper record of test rotor running history for up to 16 parameters. This provides backup records in case of a Pacific system malfunction. Note that the sample rate on this system is not fast enough to register any transient pulses from the EM flux Detector.

EM Flux Detection Instrumentation

54. The *EM flux Detector* is a custom signal detector circuit designed and fabricated by PSEF to provide an output signal to the APEX high speed data acquisition system for indication and recording of the "HEEMFG Effect". The detector circuit converts the "HEEMFG Effect" ac voltage signal output by the radio frequency (RF) receiving antenna surrounding the test article to a voltage proportional to relative amplitude. The detector's output is transitioned smoothly to a purely dc value above 100kHz for compatibility with the APEX data system. The signal is pure ac below 25kHz and a combination of ac riding on dc between 25kHz to 100kHz. It can detect continuous sinusoidal RF wave voltage signals over an ultra-wide 3 Hz to 3.2 GHz frequency band and RF wave bursts greater than .5 μsec in duration. The sensitivity (gain) is non-linear with notch attenuations throughout the bandwidth. The design intent is to have the EM flux detector output at least 2 volts dc for very low power level ac signals from the antenna, in the range of .1 to 50 milliwatts. **Note that the portion of signal cable connecting the EM flux Detector to the antenna outside the spin chamber will need to be EMI shielded.**

55. A *Receiving Antenna* was designed and fabricated by PSEF to receive RF waves emitted by the rotating test article capacitor for detection by the EM flux detector circuit. It is designed to receive RF waves from 3 Hz to 3.2GHz, but sensitivity is greatly reduced below 300 Hz. The receiving antenna consists of a wire wound plastic (delrin) mandrel installed inside the spin chamber so it surrounds the test article. The antenna is bolted to and pilots on the bottom surface of the proximity probe mount so it is positioned concentric with the capacitor. The plastic mandrel is non-conductive and transparent to RF waves. Multiple layers of small gauge magnet wire (38 to 30 gauge) are wrapped around a nominal 11/16"

diameter mandrel of .06” radial wall thickness. Radial clearance with the test vehicle is .06” and radial distance from the magnet wire wrap to the OD of the capacitor is .2”.

56. An *EMI Shielded Signal Cable* is required between the EM flux detector located on spin chamber #4 (room 72) and the APEX high speed data system in the control room (room #81). A single run of about 125 ft. of Belden 9841, 2 conductor twisted shielded pair, 24 AWG size, stranded cable routed inside EMI shielding flexible conduit is required. These shielding precautions are needed to ensure EMI does not interfere with the EM flux detector’s output causing false positive indications of the HEEMFG effect. Connection of the signal cable ground is to be connected to the spin chamber.

57. An *APEX High Speed Data Acquisition System* will record the EM flux detector output signal for primary indication of the presence of the HEEMFG Effect. This system is being used for its high sample rate and ease of storing and viewing large data files. The system will be set to record at its maximum sample rate of 200k samples/sec (1 sample every 5 µsec). The APEX system will record EM Flux relative amplitude as a DC voltage versus time. The system can only resolve the frequency of EM flux signals below 100 kHz; above 100 kHz, only relative amplitude will be indicated with no frequency information.

58. *Signal Generators:* Two signal generators will be used to supply simulated signals during bench testing of the EM flux detector and antenna performance over the very wide 3 Hz to 3.2 GHz frequency band of interest. For low frequencies, an Agilent model 33220A 20 MHz Function/Arbitrary Waveform Generator will be used. An Agilent model 8648C 9kHz – 3200 MHz Signal Generator has been rented for $310/month to cover the high frequency requirements.

59. Oscilloscope: A Tektronix model TDS 2014C Digital Storage O-scope, 100 MHz, 2GS/s will be used to measure the output signal of the EM Flux Detector/Antenna during bench testing.

Instrumentation Parameters List

60. The list of parameters and data system connections required for safe operation of the test is given in tables 4. A subset of these parameters will be recorded on a paper chart recorder; the chart recorder configuration is given in table 5.

Table 4–Instrumentation List

HEEMFG Spin Test
Instrumentation Parameters List
(4 June 2018, rev. 1)

Description	Parameter Label	Measurement Range	Units	*Shutdown Limit S.P.*	DCS	PACIFIC (10 Hz)	APEX (200 kHz)	Chart Recorder	Tach Display	BSI Control
SYSTEM TIME SYNC										
IRIG-B time sync	IRIG					X	X	X		
ROTATIONAL SPEED										
Speed	Speed_(krpm)	0 - 110	krpm	*> 102*	X	X	X	X		
Speed at 0°	Speed1_(krpm)	0 - 110	krpm		X*	X				X*
Speed at 120°	Speed2_(krpm)	0 - 110	krpm		X*	X			X*	
Speed at 220°	Speed3_(krpm)	0 - 110	krpm		X*	X				
DISPLACEMENT (VIBRATION)										
Spindle Displacement X	Disp_X_(mils-PtP)	0 - 50	mils_PtP	*> 30*	X	X	X	X		
Spindle Displacement Y	Disp_Y_(mils-PtP)	0 - 50	mils_PtP	*> 30*	X	X	X	X		
Spindle Displacement X raw	Disp_X_raw_(mils)	+ / - 25	mils			X*	X*			
Spindle Displacement Y raw	Disp_Y_raw_(mils)	+ / - 25	mils			X*	X*			
CHAMBER CONDITIONS										
Chamber Vacuum	Vacuum_(torr)	0 - 2	torr	*> 2*		X	X	X		
Chamber Air Temperature	T_ChamAir_(F)	0 - 200	°F	*>150*		X	X	X		
"HEEMFG EFFECT" SENSOR										
EM Field Flux Detector	**EMF_Flux_(V)**	**0 - 10**	**V**				**X**			
AIR MOTOR										
Supply Oil Temperature	T_SupplyOil_(F)	0 - 200	°F	*> 150*		X				
Return Oil Temperature	T_ReturnOil_ (F)	0 - 200	°F	*> 175*		X				
Bearing Oil Pressure	P_BrgOil_(psig)	0 - 50	psig	*<10*		X				
Damper Oil Pressure	P_DamperOil_(psig)	0 - 50	psig	*<10*		X				
Supply Balance Air Pressure	P_SupplyBalAir_(psig)	0 - 50	psig			X				
Seal Air Pressure	P_SealAir_(psig)	0 - 50	psig			X				
Drive Air Pressure	P_DriveAir_(psig)	0 - 150	psig			X		X		
Brake Air Pressure	P_BrakeAir_(psig)	0 - 150	psig			X		X		
VACUUM PUMP										
Vacuum Pump Oil Temperature	T_VacPump_Oil_(F)	0 - 200	°F			X				
NOTES:										
X* indicates raw signal										

Table 5–Chart Recorder Setup

HEEMFG Spin Test
Chart Recorder Layout
(4 June 2018 rev.1)

Graph	Parameter	Display Range	Units	Unit Grad.	Text	Description	Graph Size
n/a	n/a: Label Header	n/a	n/a	n/a	"HEEMFG Spin Test "		n/a
n/a	n/a: IRIG	n/a	n/a	n/a	Time/Date on edge of strip chart	IRIG-B time code sync from Datum model 9300 Time Code Generator	n/a
1	Speed_(krpm)	0 - 110	krpm	2 2	*Speed_(krpm) 0 - 110*	Speed, median value from Speed 1, Speed2, and Speed3	1/4
2	~~EMF_Flux_(V)~~	~~0 - 10~~	~~krpm~~	~~0 2~~	~~*EMF_Flux_(V) 0 - 10*~~	~~EM Field Flux Detector Output~~	1/4
3	DISP_X_(mils-PtP) DISP_Y_(mils-PtP)	0 - 50 0 - 50	mils-PtP mils-PtP	1	*DISP_X_(mils-PtP) 0 - 50* *DISP_Y_(mils-PtP) 0 - 50*	Spindle X radial displacement ~ 1 25" from spindle end Spindle Y radial displacement ~ 1 25" from spindle end	1/8
4	Vacuum_(torr)	0 - 2	torr	0 04	*Vacuum_(torr) 0 - 2*	Chamber Vacuum	1/8
5	T_ChamAir_(F)	0 - 200	°F	4	*T_ChamAir_(F) 0 - 200*	Chamer Air Temperature measured near spindle	1/8
6	P_DriveAir_(psig) P_BrakeAir_(psig)	0 - 150 0 - 150	psig psig	3	*P_DriveAir_(psig) 0 - 150* *P_BrakeAir_(psig) 0 - 150*	Drive pressure measured at Air Motor port Brake pressure measured at Air Motor port	1/8

METHOD OF TEST

61. The spin test will be conducted fully manned, one shift per day, to execute the test matrix (table 2); each test may need to be run multiple times to establish repeatability. Completing the test matrix will require 3 to 10 test days. Tests will be run with air motor compressed air supply pressure set to 70 psig. The Pacific system in single scan mode will record all the test runs for each day in a single date stamped text file. The APEX system will record individual test runs as separate data files with a date and sequential run number embedded in the filename.

62. Testing will be conducted in stages as described in test run procedures below:

Test Run Procedures

63. *Stage 1 - EM Flux Detector/Antenna Performance Evaluation in Spin Chamber:* The EM flux detector with antenna will be installed in the spin chamber environment to evaluate the un-calibrated response over the 3 Hz to 3.2kHz bandwidth. A dummy capacitor (aluminum spacer) test vehicle will be installed in the air motor and the spin chamber evacuated. The proximity probes will be powered off and the cable ends stowed in EMI shielded box; all other facility instrumentation will be powered on. The APEX system will be set up to monitor and record EM flux voltage versus time. The EM flux background noise level will be determined by recording a 30 second history of EM Flux voltage versus time - it's expected to be less than .25 volts. For this testing, **the HEEMFG effect detection threshold level is defined as .25 volts above the EM flux detector background noise level**.

64. Next, a signal generator lead will be connected to the dummy capacitor via the set screw on the capacitor test vehicle. The signal generator will supply an ac signal to the dummy capacitor causing it to emit RF waves simulating the HEEMFG effect. The frequency of this simulated HEEMFG effect will be swept over the entire bandwidth, with signal strength adjusted as required (.1 to 50 milliwatts maximum),

to produce an EM flux detector output observed on the APEX system above the detection threshold level. The frequencies where this minimum detection threshold is not met will be documented. This same procedure shall be repeated with the proximity probes turned on. This procedure is estimated to require about 1 to 1.5 shifts.

65. *Stage 2 – Air Motor Functional Checkout and Speed Controller Tuning:* This stage of the test will be run with just the modified threaded spindle installed. An antenna is not installed for these test runs. One proximity probe (X direction) is powered on. The purpose is to a) perform a functional check out the control system; b) determine the amplitude and frequency (by observing FFT) of spindle radial displacement levels; c) tune the control system for the mission cycles over the entire 0 to 100,000 rpm running range; and d) establish the high end overspeed trip setpoint value necessary to keep the air motor from exceeding the 105,000 rpm turbine rotor limit during maximum acceleration.

66. *Stage 3 – Trial Running of Test Vehicle with Dummy Capacitor to Determine Max Speed Capability:* This stage of testing will evaluate the test vehicle's ability to withstand the centrifugal loading (proportional to speed squared) induced during spinning. This test will be run with a dummy capacitor (aluminum spacer) test vehicle installed, an antenna blank mandrel installed, and one proximity probe (X direction) powered on. The test vehicle will be accelerated at 5000 rpm/s to a target speed of ~50,000 rpm, dwell for at least 6 minutes, decelerated at 5000 rpm/s to 0 rpm, and then visually inspected. Replace test vehicle if damaged. Based on the condition of the test vehicle, the target speed will be incremented up or down, and the test repeated until the max safe speed is determined.

67. Next, the test vehicle's ability to handle air motor maximum accel/decel rates will be evaluated by performing at least ten saw-tooth cycles from 0 rpm to test vehicle max speed and back to 0 rpm at maximum acceleration/deceleration. The test vehicle will be visually inspected. If the test vehicle is damaged, repeat test at half the accel/decel rates.

68. *Stage 4 - Trial Running of Dummy Capacitor Test Vehicle to Establish EM Flux Baseline Noise Level:* This test will be run with a dummy capacitor (aluminum spacer) test vehicle installed, an antenna installed, and proximity probes powered off and the cable ends stowed in the spin lid mounted EMI shielding box. The APEX system will be set up to monitor and record EM flux voltage and speed versus time. With the test vehicle static, a 30 second recording on APEX will establish the static EM flux baseline noise level. Next, test runs will include a stair step to test vehicle max speed (follow stage 3 procedure), a 500 rpm/s slow sweep from 0 to test vehicle max speed to 0 rpm , the mission cycle with low acceleration rates, and the mission cycle with high acceleration rates, with speed setpoints limited to test vehicle max speed determined in stage 3 procedures. The APEX system will record the EM flux detector output generating an EM flux baseline for each test run; the noise levels should be the same for all of the baseline runs.

69. *Stage 5 – Spin Test of Charged Capacitor to Evaluate HEEMFG Effect:* A series of tests will be run using a fully charged capacitor to evaluate the HEEMFG Effect. A new capacitor will be prepared using the Capacitor Pre-Test Preparation, Capacitor Load Test, and Capacitor Test Vehicle Assembly procedures given below. These tests will be run with a capacitor test vehicle and antenna installed. The proximity probes will be powered off and the cable ends stowed in the spin lid mounted EMI shielding box. The APEX system will be set up to monitor and record the EM flux signal for each test run.

70. With the test vehicle static, a 30 second recording on APEX will establish the static EM flux baseline noise level. Next, test runs will include a stair step run-up to test vehicle max speed to determine the capacitor's max speed capability. The test vehicle will be accelerated at 5000 rpm/s to a target speed of ~50,000 rpm, dwell for at least 6 minutes, decelerated at 5000 rpm/s to 0 rpm, and then load test the capacitor in place with antenna removed. Replace the capacitor if it fails the test and reinstall the antenna. Based on the condition of the capacitor, the target speed will be incremented up or down, and the test repeated until the capacitor max speed is determined. If there is any indication of the HEEMFG effect during this test run, repeat test and investigate; otherwise continue with test matrix runs.

71. Once the capacitor maximum speed has been determined, the following test runs will be performed with test vehicle speed set points limited to the capacitor max speed value. A capacitor load check will be performed after each run. The remaining runs include a 500 rpm/s slow sweep from 0 to capacitor max speed to 0 rpm; a mission cycle profile with low acceleration rates; a mission cycle with high acceleration rates; and both mission cycle profiles modified with the fastest achievable acceleration and deceleration rates determined in stage 2 test runs.

72. The following procedures will be used to prepare the capacitor for test runs, to load test capacitor before and after test runs, and to build up a capacitor test vehicle:

Capacitor Pre-Test Preparation Procedure

1. Remove the solder tabs from a new capacitor.
2. With fine tip sharpie marker, add an ID number to the capacitor surface for future reference.
3. Inspect capacitor surfaces for damage or deformation created during solder tab removal.
4. If damaged, discard capacitor.
5. Fully charge the capacitor.
6. Perform constant current load test (procedure TBD) on capacitor.
7. Measure and record the capacitor voltage with capacitor ID.
8. Capacitor is ready for installation into capacitor test vehicle.

Capacitor Load Test Procedure

1. TBD.

Capacitor Test Vehicle Assembly

1. Apply Loctite 425 threadlocker to capacitor holder #4-40 threads.
2. Install set screw into holder with cone point on outside (use .05" hex screwdriver).
3. Position set screw axially so hex key side is .002 to .005" above holder inside surface.
4. Install capacitor or dummy (aluminum spacer) into holder with negative (-) side down.
5. Verify electrical continuity of capacitor with set screw.
6. Create a nylon spacer from .06" thick nylon sheet using a 17/64 hand punch.
7. Install .06" thick nylon spacer into holder against capacitor.
8. Apply Loctite 425 threadlocker to spindle 5/16"-24 external threads.
9. Install holder onto spindle.
10. Apply 30 lb-in to holder hex feature using screwdriver style torque wrench (0-100 lb-in).
11. Verify capacitor voltage at set screw (-) and holder test leads hole.
12. Test vehicle is ready to run.

Test Operations

73. Test operations are covered by the Daily Checklist given in Appendix C and the Emergency Procedures found in Appendix D.

OPERATING LIMITS AND ALARMS

74. Operating limits for the air motor and drive spindle are given in table 6 below.

Table 6. Operating Limits

Rotational Speed (rpm)	105,000
Air Motor Damper Oil Pressure (psig)	< 10
Air Motor Bearing Oil Pressure (psig)	< 20
Air Motor Return Oil Temp (°F)	> 180
Vacuum (torr)	< 20
Drive Spindle Radial Displacement (mils P-P)	30
Cycle Timer	disabled

DATA REDUCTION PROGRAMMING AND ANALYSIS

75. The EM flux detector provides a go/no-go output for the indication of the HEEMFG effect. The only post processing of test data required will be to plot EM flux and speed parameters versus time data plots using Excel for a final report.

REPORTING REQUIREMENTS

76. The planned deliverables consist of:

a) *email test status reports*, completed daily by the test engineer, during test operations or upon the occasion of a significant test event;

b) *a test log she*et maintained by the test technician to include, test conditions, dates and times as well as notes detailing significant events and reasons for shutdowns;

c) *a final test report,* completed by the test engineer, describing the test methods and test results.

TEST RESULTS (Preliminary Draft)

77. A charged disk test article, in the form of a coin cell capacitor, was spin tested to evaluate the presence of the HEEMFG Effect. Six days of testing were conducted from 18 through 27 September 2018 in the Rotor Spin Facility, spin chamber #4. The testing was performed in 5 stages generally following the test plan test matrix (table 2).

78. Stage 1: On 18 September, the *EM Flux detector/antenna performance was evaluated* as installed in the spin chamber 4. Detection of the HEEMFG Effect is accomplished by recording the EM Flux detector output on the APEX data system at 200 kHz sample rate and looking for signal increases above the noise level. This static evaluation test used a dummy capacitor (aluminum spacer) test vehicle and a receiver antenna manufactured with two layers of 34-gauge magnet wound around the antenna mandrel. The proximity probes used to monitor spindle displacement were powered off and disconnected with the lead ends coiled up in a metal box on the spin chamber to avoid Electro-Magnetic Interference (EMI).

79. A signal generator supplied a 14.5 dBm (28 milliwatts) maximum level ac signal to the dummy capacitor test vehicle set screw via a signal cable passing through the spin lid; together, the uninsulated cable end and dummy capacitor acted as a transmitting antenna to radiate RF energy into the receiver antenna generating a simulated "HEEMFG Effect" signal from the EM flux detector. The EM flux detector's noise level was nominally positive 2.2 volts as measured on the APEX's 10-volt maximum input. The EM Flux detector output was evaluated at 19 discreet frequencies from .02 MHz to 3200 MHz and recorded as APEX run 7. The effect of powering proximity probes was evaluated at 333 and 1100 MHz as APEX runs 8 and 9. The results are tabulated below (table 7) in the order they were tested:

Table 7 – EM Flux Detector/Antenna In-Chamber Performance Evaluation Results

Frequency (MHz)	**EM Flux Detector Response (volts)**	**Comment**	**Proximity Probes**	**APEX Run #**
No input	2.2	Baseline noise level (electronics warmed up)	Off and EMI shielded	7
20, 50, 100, 200, 333, 400, 500, 750	>=10 (saturated)	good signal	Off and EMI shielded	7
1100	3.6	good signal	Off and EMI shielded	7
1750	5.76	good signal	Off and EMI shielded	7
2550	none	Signal below noise level	Off and EMI shielded	7
2700	2.5	good signal	Off and EMI shielded	7
2900	5.4	good signal	Off and EMI shielded	7
3200	none	Signal below noise level	Off and EMI shielded	
10	5.26	good signal	Off and EMI shielded	7
1, .5 , .1, .02	none	Signal below noise level	Off and EMI shielded	7
333	10	Probes are interfering	On –single probe	8
333	9.9	Probes are interfering	On – two probes	8
1100	8.9	Probes are interfering	On –single probe	9

1100	9.9	Probes are interfering	On – two probes	9

80. This was a very imperfect test with results influenced by the characteristics and positioning of the signal cable used to pass through the spin lid and connect to the capacitor test vehicle; it's the best that could be done with the equipment available. A non-response to a frequency input does not mean the EM Flux detector/antenna is not working, as the detector/antenna has been designed to respond to frequencies in the 3 Hz to 3.2 GHz bandwidth of interest.

81. Despite care taken to shield the EM Flux detector circuits from external EMI, it was found that keying the transmit button on a walkie-talkie held in close proximity to the spin chamber caused the EM Flux detector to output a high level on the APEX system. This fact was exploited to insert a mark in the APEX data record before and after each test frequency.

82. These static tests confirmed the EM Flux Detector/Antenna is working as designed and that the proximity probes need to be powered off during HEEMFG Effect measurement to prevent EMI from influencing the output.

83. Stage 2: On 19 September, the *Air Motor functional checkout and speed controller tuning* was performed; a receiver antenna was not installed. High synchronous spindle displacement levels were experienced during initial running of the air motor to a maximum of 40 krpm under manual control; the spindle (#1) was determined to be bowed and a spare straight spindle (#2) was swapped in. A run to 81 krpm showed the displacement levels were reduced in amplitude and sub-synchronous which is in line with prior running experience; the straight spindle resolved the problem.

84. On 20 September, air motor checkout runs resumed, running up to 100 krpm in stair step speed increments under manual control. Switching to automated control, this was followed by short saw tooth cycles (15k to 100k to 15k rpm) to tune the cycle controller. After a handful of cycles, at 69 krpm, the displacement limit (speed dependent) was exceeded (barely) and the DCS system shut down the test; several restart attempts resulted in displacement limit trips at progressively lower speeds.

85. Tear down and inspection of the air motor revealed failed bearings, damage to the rotor, and the spindle was discolored from high temperature. Review of the data showed all other facility parameters were within normal limits leading up the failure. No definitive root cause was established other than to speculate that prior running with the bowed spindle damaged the bearings and led to the failure.

86. Over the next several days, the air motor was rebuilt with new bearings, a rotor (previously repaired), and a new spindle (#3).

87. On the afternoon of 25 September 2018, the air motor checkout runs were completed under manual control with a run to 100 krpm in stair step speed increments followed by a stair step run-up to 86 krpm with dwell time up to 6 minutes at each increment.

88. Stage 3: On the afternoon of 25 September, the *trial running of test vehicle with dummy capacitor (aluminum spacer*) was begun to determine maximum speed capability of the capacitor test vehicle to withstand the centrifugal loads induced during spinning and whether the radial clearance between the rotating test vehicle and static antenna is sufficient to avoid contact. To avoid damage to the custom manufactured antenna from a high displacement level or failed test vehicle, a blank antenna mandrel was installed.

89. The capacitor holder survived 60 krpm for 6 minutes without backing off the spindle but some of the thread-locker was thrown onto the inside of the antenna mandrel; the thread-locker had been given only about 20 minutes to cure (OEM recommends 24 hour for full cure). Match marks were added to the capacitor holder and the spindle using sharpie marker to make relative rotation easily recognized. A subsequent run to 86 krpm for 4 minutes caused the capacitor holder to back off 1/2 turn. Both times, the antenna mandrel was warm to the touch. The capacitor holder and spindle threads were cleaned and the threadlocker was reapplied and allowed to cure overnight.

90. On the morning of 26 September, trial running of the capacitor holder with aluminum spacer continued, but with the top speed limited to 86krpm (75% stress of 100 krpm) in an effort to minimize the risk of damage to the air motor from a repeat air motor bearing failure and/or capacitor holder failure. A six minute dwell (APEX run 17) under manual control and a 25 cycles (10k-86k-10k rpm) in 7 minutes run (APEX run 18) under automated control were completed. The capacitor holder did not back off the threads this time - likely due to the overnight cure time for the thread locker.

91. Stage 4: On the afternoon of 26 September, the *trial running of test vehicle with dummy capacitor (aluminum spacer) to establish the EM Flux baseline noise level* was begun. The antenna that was evaluated in stage 1 static tests was installed for this testing. The EM Flux detector baseline runs up to speeds of 86 krpm were completed successfully; they included a slow acceleration, six minute dwell, 25 cycles (10k-86k-10k rpm) in 7 minutes, mission cycle low, mission cycle high, and 25 cycles (10k-86k-10k rpm) in 5 minutes. The EM flux detector output was recorded in one file as APEX run #20.

92. Three capacitors were charged (A, B, and C) to verify that they had at least 4 coulombs of charge; they were assembled onto spindles #3, #4, and #5 respectively for overnight cure of the thread locker in preparation for stage 5 tests.

93. **Stage 5:** On 27 September, the **Spin Test of a Charged Capacitor to Evaluate the HEEMFG Effect** was conducted using the receiver antenna evaluated in the stage 1 and stage 4 tests and spinning of three capacitors (A, B, and C) in separate test runs under vacuum of .42 torr. The capacitor test results are summarized below:

94. Capacitor A survived short duration runs to 86 krpm recorded on APEX as runs 23, 23a, 25, and 26; capacitor voltage was reduced, 1.288 (from 1.33) and a discharge test demonstrated its charge was reduced to 2.26 coulombs (from 4 coulombs); it still functions and was recharged to full capacity.

95. Capacitor B did not survive extended operation at 86 krpm recorded on APEX as runs 27-34; voltage was reduced to 1.233 (from 1.317); a discharge test demonstrated only .36 coulombs of charge remained (from 4 coulombs); it was damaged and will not take a charge.

96. Capacitor C was spun to 100 krpm for six minutes and recorded on APEX as run 26; its voltage was reduced to 1.223 (from 1.317); during a discharge test attempted the next day (28 September), the capacitor was accidently damaged; however, based on the experience with capacitor B, it was likely damaged from the spinning. Note that all of the blue thread-locker used on the capacitor holder/ spindle threaded connection was deposited on the inside of the antenna mandrel. The match marks on spindle and capacitor holder were still aligned.

97. The capacitors were subjected to peak acceleration rates of at least +/- 30 krpm/s.

98. A walkie-talkie transmitter was momentarily keyed on in close proximity to the EM Flux detector at the start and end of each test run providing confirmation in the digital record that the EM Flux detector was working at the beginning and end of each test run.

99. After each test run, it was necessary to replay and review the 200 kHz sample rate APEX recorded EM Flux detector data for indication of transient HEEMFG Effect bursts that may have escaped real-time display on the slower update rate APEX display screen.

100. Careful review of the EM Flux detector output data files showed no instances of EM Flux detector output voltage rising above the noise baseline; therefore, there was no indication of HEEMFG Effect observed for this test configuration.

DISCUSSION

101. The HEEMFG theory requires the charge to be on the surface of the disk. In the tested configuration, the charge distribution in the capacitor is not known and could not be verified. The tested configuration cannot disprove the HEEMFG theory.

CONCLUSION

102. The HEEMFG Effect was evaluated by spinning three coin cell capacitors each with 4 coulombs of charge, at speeds up to 100 krpm with acceleration rates up to 30 krpm/s and under vacuum level of .42 torr. The capacitor test vehicle and EM Flux detector/antenna performed well.

103. With the current test configuration, the HEEMFG Effect was not observed or disproved.

RECCOMENDATION

104. To continue this effort, the following test configuration changes are recommended:

- Design a charged disk test configuration that ensures the charge is at the surface of the disk;
- Improve the EM Flux detector circuit to increase sensitivity and improve shielding from external EMI;
- Improve receiver antenna design for increased sensitivity to B-fields (magnetic fields) and increased sensing area.

Appendix A (HEEMFG Article)

The high energy electromagnetic field generator

Salvatore Cezar Pais

Department of Defense/Department of the Navy,
Naval Air Systems Command/NAWCAD,
NAS Patuxent River Maryland 20670, USA
(b) (6)

Abstract: The original concept described is named the high energy electromagnetic field generator. This concept's governing physics entail the coupling of gyration (high frequency spin), vibration (high frequency abrupt pulsations/harmonic oscillations) and possible curvilinear translation, of electrically charged systems. If we couple the system's high frequency of rotation (30,000 to 100,000 RPM, and higher) with high vibration (abrupt pulsations/harmonic oscillations) frequencies in the range of 10^9 to 10^{18} Hertz (and above) we can obtain electromagnetic field intensity values in the range 10^{24} to 10^{28} Watts/m^2 (and beyond). These extremely high electromagnetic field intensity values emphasise the novelty of this concept, especially suited for the design of energy generation machinery with power output levels much higher than those currently achievable. The utilisation of such high power sources for space power and propulsion generation, as it pertains to reduction in a spacecraft's inertial mass as a direct result of local vacuum polarisation, is an important application of the described theoretical concept. In this manner, extreme spacecraft speeds can be achieved.

Keywords: faster than light travel; superluminal propulsion; quantum vacuum plasma; QVP; vacuum energy fluctuations; vacuum polarisation; spacetime manipulation; quantum vacuum engineering; quantum field theory; far from equilibrium thermodynamics; spatio-temporal excursion.

Reference to this paper should be made as follows: Pais, S.C. (2015) 'The high energy electromagnetic field generator', *Int. J. Space Science and Engineering*, Vol. 3, No. 4, pp.312–317.

Biographical notes: Salvatore Cezar Pais obtained his Doctorate in Mechanical and Aerospace Engineering from Case Western Reserve University, while working as a NASA Graduate Student Research Fellow at NASA Glen (Lewis) Research Center. His research studies deal primarily with defence-oriented work, performed as a General Engineer/Advanced Concepts Analyst at Northrop Grumman Aerospace Systems. At the present time, he works for the Department of Defense, Department of the Navy/Naval Air Systems Command at NAS Patuxent River in Maryland.

1 Introduction

The original concept described herein, is named the high energy electromagnetic field generator (HEEMFG). When put in practice, this system can provide the design of energy generation machinery with power output levels much higher than those currently achievable. The utilisation of such high power sources for space power and propulsion generation, as it pertains to reduction in the spacecraft's inertial mass as a direct result of local vacuum polarisation, is an important application of the described theoretical concept.

This concept's governing physics entail the coupling of gyration (high frequency spin), vibration (high frequency abrupt pulsations/harmonic oscillations) and possible curvilinear translation (thus three modes of motion) of electrically charged systems.

There are four known fundamental forces which control matter and therefore control energy, namely the strong and weak nuclear forces, the electromagnetic (EM) force and the gravitational force. In this hierarchy of forces, the EM force is perfectly positioned to be able to manipulate the other three. A stationary electric charge gives rise to an electric (electrostatic) field, while a moving charge generates both an electric and a magnetic field (hence, the EM field); additionally an accelerating charge induces EM radiation in the form of transverse waves, namely light. Mathematically as well as physically, EM field intensity can be represented as the product of electric field strength and magnetic field strength. EM fields act as carriers for both energy and momentum, thus interacting with physical entities at the most fundamental level.

Artificially generated, high energy, EM fields interact strongly with the vacuum energy state (an aggregate/collective state comprised of the superposition of all quantum fields' fluctuations permeating the entire fabric of spacetime), thereby giving rise to emergent physical phenomena (in other words revolutionary/new physics), such as force and matter fields unification. According to quantum field theory, this strong interaction between the fields is based on the mechanism of transfer of vibrational energy between the fields, further inducing local fluctuations in adjacent quantum fields which permeate spacetime (these fields may or may not be EM in nature). Matter, energy, and spacetime are all emergent constructs which arise out of the fundamental framework that is the vacuum, energy state.

Everything that surrounds us, ourselves included, can be described as macroscopic collections of fluctuations, vibrations, oscillations in quantum mechanical fields. Matter is confined energy, 'frozen' in a quantum of time. Therefore, under certain conditions (such as the coupling of hyper-frequency axial spin with hyper-frequency vibrations of electrically charged systems) the rules and special effects of quantum field behaviour also apply to macroscopic physical entities (O'Connell et al., 2010).

Moreover, coupling of hyper-frequency gyrational (axial rotation) and hyper-frequency vibrational electrodynamics (as used in the concept herein disclosed) is conducive to a possible physical breakthrough (force field unification is feasible with the concept at hand) in the utilisation of the macroscopic quantum fluctuations vacuum plasma field (quantum vacuum plasma – QVP, in short) as an energy source (or sink), an induced physical phenomenon, for which the technology readiness level has been considerably advanced by a team of research engineers from NASA JSC (Brady et al., 2014). This research involves the use of high radio frequency/microwave driven resonant cavity Q-thruster technology within the context of QVP physics.

The QVP is the electric glue of our plasma universe. The Casimir effect, the Lamb shift, and spontaneous emission, are specific confirmations of the existence of QVP (Milonni, 1994).

It is important to note that in region(s) where the EM fields are strongest, the more potent are the interactions with the QVP, therefore, the higher the induced energy density of the QVP particles which spring into existence(the Dirac Sea of electrons and positrons). These QVP 'particles' may augment the obtained energy levels of the HEEMFG system (even though they are short-lived, these 'virtual' particles have a real effect).

To be more precise, the EM fields created by the HEEMFG system, interact with the vacuum energy state, which is an aggregate state composed of the superposition of all quantum fields' fluctuations filling the entire fabric of spacetime. Contributions to this vacuum state energy density are made by the quantum vacuum-zero point fluctuations, the quantum chromo-dynamics gluon and quark condensates and the newly discovered Higgs field (exhibiting massive 126 GeV particles), among other yet undiscovered fields (super-symmetry). In other words, major contributions to the vacuum energy state are made by collectives of quantum fluctuations in fermionic fields (fields of matter), quantum fluctuations in bosonic fields (fields of force) and quantum fluctuations in scalar fields (Higgs field).

2 Concept novelty

The physical equation which describes the maximum intensity achieved by the HEEMFG system is described by the magnitude of the Poynting vector, which in non-relativistic form (accounting for all three modes of motion) can be written as:

$$S_{max} = f_G\left(\sigma^2 / \varepsilon_0\right)\left[R_r\omega + R_v\nu + v_R\right] \tag{1}$$

where f_G is the HEEMFG system geometric shape factor (equal to 1 for a disc configuration), σ is the surface charge density (total electric charge divided by surface area of the HEEMFG system), ε_0 is the electrical permittivity of free space, R_r is the radius of rotation (disc radius), ω is the angular frequency of rotation in rad/s, R_v is the vibration (harmonic oscillation) amplitude, ν is the angular frequency of vibration in Hertz, and the term v_R is the curvilinear translation speed (acquired via a propulsive unit of either chemical, nuclear or magneto-plasma-dynamic (VASIMR) type attached to the HEEMFG system – the integrated unit being the spacecraft).

Therefore, if we consider only rotation, given a disc configuration, with σ = 50,000 Coulombs/m^2, a disc (spinning/axially rotating) radius of 2 m and an angular speed of 30,000 RPM, we can generate an EM field intensity (S_{max} = rate of energy flow per unit area, or energy flux) value on the order of 10^{24} Watts/m^2 (this value does not account for any QVP interactions).

Furthermore, if we couple the high frequency of rotation with high vibration (harmonic oscillation) frequencies in the range of 10^9 to 10^{18} Hertz (and above) we can obtain S_{max} intensity values in the range 10^{24} to 10^{28} Watts/m^2 (and beyond). These extremely high EM field intensity values emphasise the novelty of this concept, especially suited for the design of energy generation machinery with power output levels much higher than those currently achievable.

For the case of an accelerating angular frequency of vibration ($a_{max} = R_v v^2$), neglecting rotation and curvilinear translation, equation (1) becomes (note intrinsic significance of acceleration):

$$S_{max} = f_G (\sigma^2 / \varepsilon_0)\left[(R_v v^2)\, t_{op}\right] \tag{2}$$

where t_{op} is the operational time for which the charged electrical system is accelerating.

Close inspection of equation (2) results in an important realisation, namely: strong local interaction with the high energetics of the quantum vacuum fields' fluctuations superposition (macroscopic vacuum energy state) is possible in a laboratory environment, by application of high frequency gyration and/or high frequency vibration of minimally charged objects (order of unity), in an acceleration mode. In this manner, a high degree of vacuum energy polarisation can be achieved.

Local polarisation of the vacuum in the close proximity of a spacecraft equipped with an HEEMFG system would have the effect of cohering the highly energetic and random quantum vacuum fields' fluctuations, which virtually block the path of an accelerating spacecraft, in such a manner that the resulting negative pressure of the polarised vacuum allows less laboured motion through it (Froning, 2009).

Spontaneous electron-positron pair production out of the vacuum (Schwinger, 1951; Kim, 2015) is a strong indicator of vacuum polarisation being achieved. Schwinger gives a value of the electric field (E) on the order of 10^{18} V/m for this phenomenon to take place. The mass production rate $(dm / dt)_{pp}$ of particle/anti-particle pairs can be expressed in terms of S_{max} (energy flux), namely:

$$2\gamma (dm / dt)_{pp} c^2 = S_{max} A_S \tag{3}$$

where A_S is the surface area from which the energy flux emanates, c is the speed of light in free space, and (γ) is the relativistic stretch factor $[1 - (v^2 / c^2)]^{-1/2}$. Note that the pair production rate increases with increasing energy flux from the spacecraft's generated EM field. Therefore, the level, to which the vacuum is polarised, thus allowing less laboured motion through it, strictly depends on the artificially generated EM energy flux.

If we consider the boundary condition in the close proximity of the spacecraft where the energy density of the artificially generated EM field equals the local energy density of the polarised vacuum (caused in part by the local zero-point vacuum fluctuations on the order of 10^{-15} Joules/cm^3 and in part by the artificial EM field interacting with the local vacuum energy state) we can write the approximate equivalence:

$$S_{max} (t_{op} / R_S) = \left[(h^* v_v^4) / 8\pi^2 c^3\right] \tag{4}$$

where R_S is the electromagnetic (EM) field radius at EM wave propagating time t_{op}, such that $R_S / t_{op} = c$ (where c is the light speed in free space), (h^*) is Planck's constant divided by (2π) and (ν_v) is the frequency of quantum fluctuations in the vacuum (modelled as harmonic oscillators).

Furthermore, given that the left side of equation (4) is on the order of ($\varepsilon_0 E^2$) where E is the artificially generated electric field (strength), considering the Schwinger value of (E) for the onset of spontaneous pair production, we obtain a (ν_v) value on the order of 10^{22} Hertz, which matches our expectations, since the Dirac virtual pair production, results in total annihilation, yielding gamma rays, which occupy the EM frequency spectrum of 10^{19} Hertz and above.

A recent paper (Pais, 2015) considers the possibility of superluminal spacecraft propulsion in a special relativity framework. It is observed that under certain physical conditions, the singularity expressed by the relativistic stretch factor 'gamma' as the spacecraft's speed (v) approaches the speed of light (c), is no longer present in the physical picture. This involves the instantaneous removal of energy-mass from the system (spacecraft) when the spacecraft's speed reaches (v = c / 2). The author discusses the possibility of using exotic matter (negative mass/negative energy density) to bring about this effect. This may not have to be the only alternative. The artificial generation of gravity waves in the locality of the spacecraft, can result in energy-mass removal (gravity waves are propagating fluctuations in gravitational fields, whose amplitude and frequency are a function of the motion of the masses involved).

Moreover, it is feasible to remove energy-mass from the system by enabling vacuum polarisation, as discussed by Puthoff (Puthoff, 2002; Haisch et al., 1994); in that diminution of inertial (and thus gravitational) mass can be achieved via manipulation of quantum field fluctuations in the vacuum. In other words, it is possible to reduce a spacecraft's inertia, that is, its resistance to motion/acceleration by polarising the vacuum in the close proximity of the moving spacecraft. As a result, extreme speeds can be achieved.

Think of the vacuum energy state as a chaotic system comprised of random, highly energetic fluctuations in the collective quantum fields which define it. Considering Prigogine's (1977) work on far from equilibrium thermodynamics, a chaotic system can self-organise if subjected to three conditions, namely: the system must be nonlinear, it must experience an abrupt excursion far from thermodynamic equilibrium, and it must be subjected to an energy flux (order from chaos).

An artificially generated high energy EM field can fulfil all three conditions simultaneously, when strongly interacting (especially in an accelerated vibration/rotation mode) with the local vacuum energy state. Recall that these interactions are induced by the coupling of hyper-frequency axial rotation (spin) and hyper-frequency vibration (harmonic oscillations/abrupt pulsations) of electrically charged systems (HEEMFG), placed on the outside of the spacecraft in strategic locations. In this manner, local vacuum polarisation, namely the coherence of vacuum fluctuations within the immediate proximity of the spacecraft's surface (outside vacuum boundary) is achieved, allowing for 'smooth sailing' through the negative pressure (repulsive gravity) of the void.

As an aside, force and matter fields unification (Gross, 2007) is feasible with the concept at hand, due to the extremely strong interactions (EM in nature) between ordinary matter and the QVP/vacuum energy state (interactions which exhibit extremely high energies on Planck length scales in the immediate proximity of the disc/spacecraft surface).

3 Conclusions

This original concept, which may represent a breakthrough technology, does reveal a novel approach to the design of energy generation machinery with power output levels much higher than those currently achievable by conventional means.

The utilisation of such high power sources for space power and propulsion generation, as it pertains to reduction in the spacecraft's inertial mass as a direct result of

local vacuum polarisation, is an important application of the described theoretical concept. In this manner, extreme spacecraft speeds can be achieved.

To be more exact, the concept at hand can be utilised in the design of a device to manipulate/modify the local spacetime lattice (topology) energy density, which can be achieved via local vacuum energy polarisation. Moreover, due to the nature of the 'emergent physics' involved, it is possible to experience spatio-temporal displacement (excursion) effects.

Disclaimer

The views espoused and conclusions reached in this technical paper are the author's own, and do not necessarily reflect the views or beliefs of the US Government and the Department of the Navy.

References

Brady, D.A. et al. (2014) 'Anomalous thrust production from an RF test device, measured on a low thrust torsion pendulum', *AIAA/ASME/SAE/ASEE Joint Propulsion Conference*, AIAA 2014-4029.

Froning, H.D. (2009) 'Quantum vacuum engineering for power and propulsion from the energetics of space', Presented at the *Third International Conference on future Energy*, Washington DC, 9–10 October.

Gross, D. (2007) *The Coming Revolutions in Theoretical Physics*, The Berkley Center for Theoretical Physics Lecture Series, 19 October, UC Berkley.

Haisch, B., Rueda, A. and Puthoff, H.E. (1994) 'Inertia as a zero-point field Lorentz force', *Phys. Rev. A*, Vol. 49, No. 2, p.678.

Kim, S.P. (2015) 'On vacuum polarization and schwinger pair production in intense lasers', *23rd International Laser Physics Workshop (LPHYS'14), Journal of Physics: Conference Series*, Vol. 594, p.012050.

Milonni, P.W. (1994) *Quantum Vacuum: An Introduction to Quantum Electrodynamics*, Academic Press, INC., San Diego, CA.

O'Connell, A.D. et al. (2010) 'Quantum ground state and single-phonon control of a mechanical resonator', *Nature*, 1 April, Vol. 464, pp.697–703.

Pais, S.C. (2015) 'Conditional possibility of spacecraft propulsion at superluminal speeds', *Int. J. Space Science and Engineering*, Vol. 3, No. 1, pp.89–92 (peer-reviewed).

Prigogine, I. (1977) *Time, Structure and Fluctuations*, Nobel Lecture, 8 December, Sweden.

Puthoff, H.E. (2002) 'Polarizable-vacuum (PV) approach to general relativity', *Foundations of Physics*, June, Vol. 32, No. 6, pp.927–943.

Schwinger, J. (1951) 'On gauge invariance and vacuum polarization', *Phys. Rev.*, Vol. 82, No. 1, p.664.

Appendix B (Capacitor Specs)

VISHAY
www.vishay.com

196 HVC ENYCAP™
Vishay BCcomponents

Hybrid Energy Storage Capacitors

Image is not to scale

FEATURES

- Polarized energy storage capacitor with high capacity and energy density
- Voltage flexibility: 1.4 V (single cell) to 2.8 V / 4.2 V / 5.6 V / 7.0 V / 8.4 V (multiple cells)
- Available in stacked through-hole (STH, radial), surface-mount flat (SMF) and lay flat configurations (LFC) with wire and connectors
- Useful life: up to 2000 h at 85 °C
- No cell balancing necessary
- Soft and low transient-voltage-controlled charging characteristic
- Non-hazardous electrolyte
- Maintenance-free, no service necessary
- Evaluation kits for engineering are available under ordering code: MAL219699001E3
- Material categorization: for definitions of compliance please see www.vishay.com/doc?99912

APPLICATIONS

- Power backup for memory controller, flash backup, RAID systems, SRAM, DRAM
- Power failure and write cache protection for enterprise SSD and HDD
- Real time clock power source
- Burst power support for flash lights, wireless transmitters
- Backup power for industrial PC's and industrial controls
- Storage device for energy harvesting
- Emergency light and micro UPS power source

MARKING

The capacitors are marked with the following information:

- Rated capacitance (in F)
- Rated voltage (in V)
- Date code
- Negative / positive terminal identification

PACKAGING

Supplied in ESD trays only

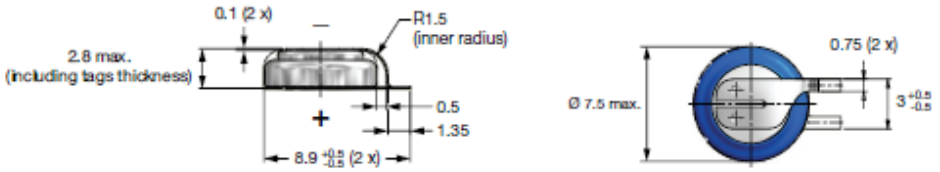

Fig. 5 - **Form D1:** Surface Mount Flat (single cell, keyed polarity)

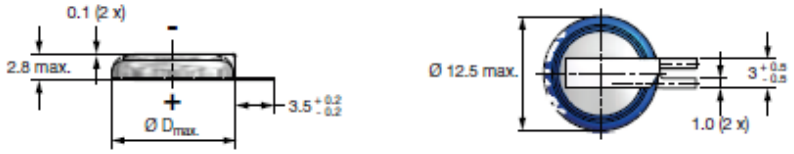

Fig. 6 - **Form D2:** Surface Mount Flat (single cell, keyed polarity)

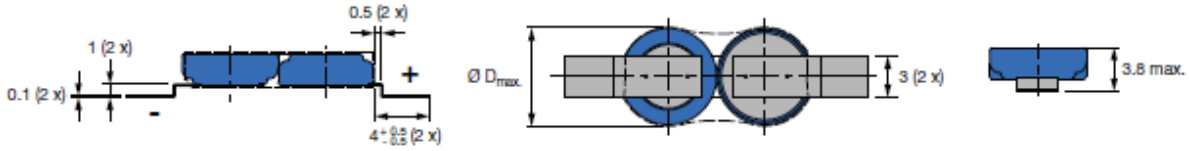

Fig. 7 - **Form E2:** Surface Mount Flat

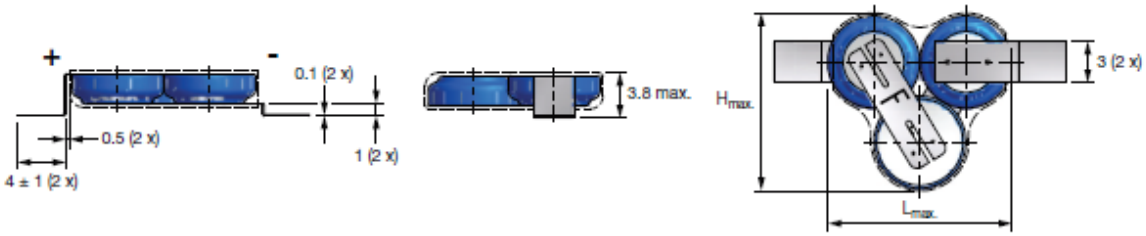

Fig. 8 - **Form E3:** Surface Mount Flat

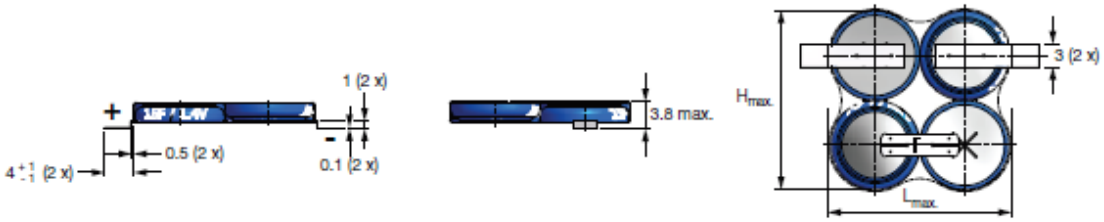

Fig. 9 - **Form E4:** Surface Mount Flat

ELECTRICAL DATA AND ORDERING INFORMATION

U_R (V)	C_R (F)	NOMINAL CASE SIZE Ø D x L D x L x H (mm)	CASE CODE	FORM	F (mm)	F1 (mm)	UCT (°C)	I_L 24 h (mA)	ESR AC [1] 1 kHz (Ω)	ESR DC [2] (Ω)	MIN. STORAGE ENERGY (Ws)	PACKAGING QUANTITIES	ORDERING CODE
SURFACE MOUNT FLAT CONFIGURATION (SMF)													
1.4	4	7.0 x 7.0 x 2.5	2 pin	C	-	-	70	0.03	2.5	7.5	4.6	50	MAL219691131E3
1.4	15	12.0 x 12.0 x 2.5	2 pin	C	-	-	85	0.12	0.6	2.5	17.5	100	MAL219691231E3
1.4	4	7.0 x 7.0 x 2.5	2 pin	D1	-	-	70	0.03	2.5	7.5	4.6	50	MAL219691141E3
1.4	15	12.0 x 12.0 x 2.5	2 pin	D2	-	-	85	0.12	0.6	2.5	17.5	100	MAL219691241E3
2.8	4	7.0 x 14.0 x 2.5	2 pin	E2	-	-	70	0.03	5.0	15.0	9.2	50	MAL219691152E3
2.8	15	12.0 x 24.0 x 2.5	2 pin	E2	-	-	85	0.12	1.2	5.0	35.0	50	MAL219691252E3
4.2	4	13.0 x 14.0 x 2.5	3 pin	E3	-	-	70	0.03	7.5	22.5	13.8	70	MAL219691153E3
4.2	15	22.0 x 24.0 x 2.5	3 pin	E3	-	-	85	0.12	1.8	7.5	52.5	35	MAL219691253E3
5.6	4	14.0 x 14.0 x 2.5	4 pin	E4	-	-	70	0.03	10.0	30.0	18.4	70	MAL219691154E3
5.6	15	24.0 x 24.0 x 2.5	4 pin	E4	-	-	85	0.12	2.4	10.0	70.0	35	MAL219691254E3
LAY FLAT CONFIGURATION (LFC)													
1.4	15	14.5 x 12.0 x 2.5	2 pin	F	-	-	85	0.12	0.6	2.5	17.5	40	MAL219691261E3
2.8	15	14.5 x 24.0 x 2.5	2 pin	F	-	-	85	0.12	1.2	5.0	35.0	40	MAL219691262E3
4.2	15	14.5 x 36.0 x 2.5	2 pin	F	-	-	85	0.12	1.8	7.5	52.5	40	MAL219691263E3
5.6	15	14.5 x 48.0 x 2.5	2 pin	F	-	-	85	0.12	2.4	10.0	70.0	20	MAL219691264E3
7.0	15	14.5 x 60.0 x 2.5	2 pin	F	-	-	85	0.12	3.0	12.5	87.5	20	MAL219691265E3
8.4	15	14.5 x 72.0 x 2.5	2 pin	F	-	-	85	0.12	3.6	15.0	105.0	20	MAL219691266E3
STACKED THROUGH HOLE OVAL													
2.8	45	25 x 15 x 5.0	3 pin	I	5	10	85	0.15	0.5	1.0	100.0	30	MAL219690203E3
4.2	45	25 x 15 x 7.5	3 pin	I	7.5	10	85	0.15	0.75	1.5	150.0	30	MAL219690201E3
5.6	45	25 x 15 x 10.0	3 pin	I	10	10	85	0.15	1.0	2.0	200.0	30	MAL219690202E3
1.4	90	35 x 25 x 5.0	3 pin	G	5	10	85	0.5	0.015	0.045	115.0	25	MAL219690106E3
2.8	90	35 x 25 x 7.5	3 pin	G	7.5	10	85	0.5	0.03	0.090	230.0	25	MAL219690103E3
4.2	90	35 x 25 x 10.0	3 pin	G	10	10	85	0.5	0.04	0.135	345.0	25	MAL219690101E3
5.6	90	35 x 25 x 15.0	3 pin	G	12.5	10	85	0.5	0.06	0.180	460.0	25	MAL219690102E3
7.0	90	35 x 25 x 17.5	3 pin	G	17.5	10	85	0.5	0.075	0.225	575.0	25	MAL219690107E3
8.4	90	35 x 25 x 20.0	3 pin	G	20.0	10	85	0.5	0.09	0.270	690.0	25	MAL219690108E3
STACKED THROUGH HOLE OVAL HORIZONTAL													
2.8	45	25 x 15 x 5.0	3 pin	K	15	10	85	0.15	0.5	1.0	100.0	30	MAL219690213E3
4.2	45	25 x 15 x 7.5	3 pin	K	15	10	85	0.15	0.75	1.5	150.0	30	MAL219690211E3
5.6	45	25 x 15 x 10.0	3 pin	K	15	10	85	0.15	1.0	2.0	200.0	30	MAL219690212E3
1.4	90	35 x 25 x 5.0	3 pin	H	25	10	85	0.5	0.015	0.045	115.0	25	MAL219690116E3
2.8	90	35 x 25 x 7.5	3 pin	H	25	10	85	0.5	0.03	0.090	230.0	25	MAL219690113E3
4.2	90	35 x 25 x 10.0	3 pin	H	25	10	85	0.5	0.04	0.135	345.0	25	MAL219690111E3
5.6	90	35 x 25 x 15.0	3 pin	H	25	10	85	0.5	0.06	0.180	460.0	25	MAL219690112E3
7.0	90	35 x 25 x 17.5	3 pin	H	25	10	85	0.5	0.075	0.225	575.0	25	MAL219690117E3
8.4	90	35 x 25 x 20.0	3 pin	H	25	10	85	0.5	0.09	0.270	690.0	25	MAL219690118E3

Notes
(1) ESR AC 1 kHz are typical values
(2) ESR DC are typical values

Table 3

LOAD CURRENTS AND VOLTAGES

C_R (F)	RECOMMENDED CHARGE CURRENT	MAX. CHARGE CURRENT	MAX. DISCHARGE CURRENT	LOWEST DISCHARGE VOLTAGE [1]
4	2 mA to 8 mA	14 mA	25 mA	n x 0.8 V
15	5 mA to 20 mA	50 mA	70 mA	n x 0.8 V
45	30 mA to 300 mA	0.5 A	0.5 A	n x 0.8 V
90	0.3 A to 1 A	1.5 A	3 A	n x 0.8 V

Note
(1) n... number of cells, permanent operation below lowest discharge voltage is not permitted

MEASURING OF CHARACTERISTICS

CAPACITANCE (C)

Capacitance shall be measured by constant current discharge method.

DISCHARGE CURRENT AS A FUNCTION OF RATED CAPACITANCE					
PARAMETER	VALUE				UNIT
Rated capacitance, C_R	4	15	45	90	F
Discharge current, I_D	4	15	45	90	mA

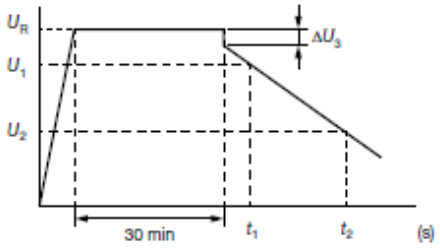

Fig. 15 - Voltage Diagram for Capacitance Measurement

Capacitance value C_R is given by discharge current I_D, time t and rated voltage U_R, according to the following equation:

C_R	Rated capacitance, in F
U_R	Rated voltage, in V
U_1	Starting voltage, in V
U_2	Ending voltage, in V
ΔU_3	Voltage drop at internal resistance, in V
t_1	Time from start of discharge until voltage U_1 is reached, in s
t_2	Time from start of discharge until voltage U_2 is reached, in s
I_D	Discharge current, in A

$$C_R(F) = \frac{I_D(A) \times (t_2(s) - t_1(s))}{U_1(V) - U_2(V)}$$

For I_D, U_1, and U_2 the following definitions have to be used:

Table 4

CAPACITANCE						
C (F)	I_D (A)	U_R (V)	U_1 (V)	U_2 (V)	t_1 (s)	t_2 (s)
4	0.004	1.4	1.3	0.7	5	> 600
4	0.004	2.8	2.7	1.9	5	> 600
4	0.004	4.2	4.0	3.1	5	> 600
4	0.004	5.6	5.4	4.4	5	> 600
4	0.004	7.0	6.7	5.6	5	> 600
4	0.004	8.4	8.1	6.9	5	> 600
15	0.015	1.4	1.3	0.7	5	> 600
15	0.015	2.8	2.7	1.9	5	> 600
15	0.015	4.2	4.0	3.1	5	> 600
15	0.015	5.6	5.4	4.4	5	> 600
15	0.015	7.0	6.7	5.6	5	> 600

CAPACITANCE						
C (F)	I_D (A)	U_R (V)	U_1 (V)	U_2 (V)	t_1 (s)	t_2 (s)
15	0.015	8.4	8.1	6.9	5	> 600
45	0.045	2.8	2.7	1.9	5	> 600
45	0.045	4.2	4.0	3.1	5	> 600
45	0.045	5.6	5.4	4.4	5	> 600
90	0.090	1.4	1.3	0.7	5	> 600
90	0.090	2.8	2.7	1.9	5	> 600
90	0.090	4.2	4.0	3.1	5	> 600
90	0.090	5.6	5.4	4.4	5	> 600
90	0.090	7.0	6.7	5.6	5	> 600
90	0.090	8.4	8.1	6.9	5	> 600

Note

- For U_2 see also Table 5

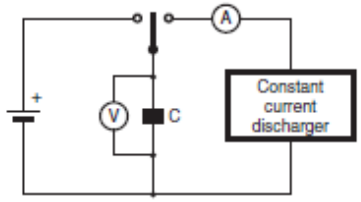

Fig. 16 - Test Circuit for Capacitance Measurement

INTERNAL RESISTANCE (R_I) AT 1 kHz

$$R_I(\Omega) = \frac{U_C(V)}{10^{-3}}$$

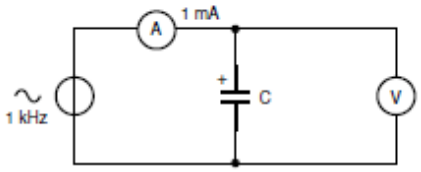

Fig. 17 - Test Circuit for R_I Measurement

LEAKAGE CURRENT (I_L)

Leakage current shall be measured after 30 min application of rated voltage U_R:

$$I_L(\mu A) = \frac{U_S(V)}{10^{-4}}$$

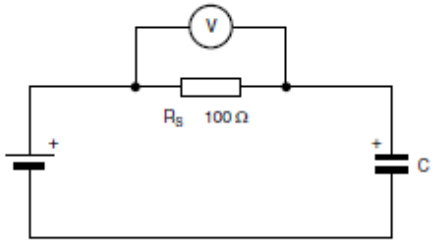

Fig. 18 - Test Circuit for Leakage Current

PRODUCT AND MOUNTING CHARACTERISTICS

Attention: parts are pre-charged at delivery - handle appropriate.

At delivery products are pre-charged and voltage over terminals is near nominal voltage. Short circuiting of product terminals is permitted. Do not short circuit permanently. Short circuiting of charged cells may heat up the cells.

For printed circuit board mounting it has to be taken into account, that for certain form factors top and bottom of products may not be insulated.

Capacitor disposal methods should be in accordance with local and state regulations.

Table 6.1

TEST PROCEDURES AND REQUIREMENTS			
NAME OF TEST	**ENYCAP TESTS SUBCLAUSE**	**PROCEDURE (quick reference)**	**REQUIREMENTS [2]**
Damp heat, steady state	4.12	500 h at 55 °C; RH 90 % to 95 %; no voltage applied	ΔC/C: ± 30 % $R_I \leq 4$ x spec. limit $I_L \leq 2$ x spec. limit
Endurance	4.13.1	T_{amb} = 70 °C / 85 °C; rated voltage U_R applied; 4.0 F, 15 F: 1000 h 45 F, 90 F: 2000 h	ΔC/C: ± 30 % $R_I \leq 4$ x spec. limit $I_L \leq 2$ x spec. limit
Useful life	4.13.2	T_{amb} = 70 °C / 85 °C; rated voltage U_R applied; 4.0 F, 15 F: 1000 h 45 F, 90 F: 2000 h	ΔC/C: ± 30 % $R_I \leq 4$ x spec. limit $I_L \leq 2$ x spec. limit
Storage at upper category temperature	4.17	T_{amb} = 70 °C / 85 °C; no voltage applied; 1000 h	ΔC/C: ± 30 % $R_I \leq 4$ x spec. limit $I_L \leq 2$ x spec. limit
Self discharge	4.1.5	24 h storage at room temperature after application of U_R for 1 h	Remaining voltage: ≥ (U_R x 0.9)
Characteristics at high and low temperature	4.19	Step 1: reference measurement at 20 °C of C, R_I, and I_L Step 2: measurement at -20 °C Step 3: measurement at +20 °C Step 4: measurement at +70 °C Step 5: measurement at +20 °C	ΔC/C: ± 30 % of +20 °C value $R_I \leq 5$ x the +20 °C value $I_L \leq 4$ x the +20 °C value
Surge voltage	4.15	Max. 30 s at room temperature U_S = n [1] x 1.6 V	No change of parameter! After surge voltage, discharge product below rated voltage

Notes

[1] n... number of cells

[2] R_I equals ESR_{AC} or ESR_{DC}

Table 6.2: Stacked Through Hole configuration (STH), Surface Mount Flat configuration (SMF), and Lay Flat configuration with Connector

TEST PROCEDURES AND REQUIREMENTS			
NAME OF TEST	**ENYCAP TESTS SUBCLAUSE**	**PROCEDURE (quick reference)**	**REQUIREMENTS [1]**
Robustness of terminations	4.4	Tensile strength; application of load force in pin / tab direction for 10 s: 10 N: for product size Ø ≥ 8 mm 5 N: for product size Ø < 8 mm	No breaks
Resistance to soldering heat	4.5	260 °C; 5 s	ΔC/C: ± 10 % R_I and $I_L \leq$ spec. limit
Solderability	4.6	Solder bath; 236 °C; 2 s; one pin immersed	≥ 75 % tinning
Vibration	4.8	10 Hz to 55 Hz; 1.5 mm; 3 directions; 2 h per direction	ΔC/C: ± 10 % R_I and $I_L \leq$ spec. limit

Notes

- Robustness - bending limited to ± 15°, force in direction of tab / pin, no twisting allowed
- Solder bath test: max. allowed case temperature during test is e.g. 85 °C or immersion of one (1) pad only
- Wave soldering allowed

[1] R_I equals ESR_{AC} or ESR_{DC}

Appendix C (Daily Checklist)

The following daily checklist has been prepared by the test technician.

INTRODUCTION

The Rotor Spin Facility (RSF), located in the Propulsion Systems Facility (BLDG 2360), performs evaluations of aircraft engines, engine accessories, and APU rotating parts and assemblies. This type of testing creates a very dangerous environment in and around the Spin Pit test chambers. Only properly trained operators and technicians can perform this type of testing.

Due to the various types of testing performed in the RSF, some items of this checklist may not be required and should be annotated “N/A”. Review the test directive and annotate or add to the checklist as necessary.

Review the test directive and identify all instrumentation and data acquisition items required for the particular test to be performed. Notify the instrumentation support branch for the set-up, calibration and the accomplishment of “end to end” checks for all required equipment prior to using this checklist.

CHECKLIST INSTRUCTIONS

1. All items of this checklist must be accomplished in sequence, unless identified “NA”.

2. Review the emergency procedures for this test to performing any test cell or equipment operation.

3. The bold lettered terms, i.e. Warning, Caution and Note, will appear throughout this checklist and must be heeded. Each term will indicate the level of additional attention required before the accomplishment of the next checklist item or section. The following is an explanation of these terms:

****WARNING**** - A failure to heed a warning may result in personal injury or death if not carefully followed or observed prior to accomplishing the next item of the checklist.

****CAUTION**** - A failure to heed a caution may result in damage to equipment if not carefully followed or observed prior to accomplishing the next item of the checklist.

****NOTE**** - A note will draw attention to an essential point prior to accomplishing the next item of the checklist.

PRE-TEST SAFETY CHECKS

1. In the RSF Control Room, ensure that all three test chamber air control switches are in the "OFF" (center) position.

2. Turn on the test in progress light for spin pit #1, and the compressor in use light for room 71.

3. Perform a walk-through of all four spin chambers and ensure that the vacuum and compressed air manifolds are intact in all four chambers. Verify that the Main Air Valves (Yellow Ball Valve) is closed in all

chambers. Verify that the vacuum manifold isolation valves, and the vacuum pump isolation valves are closed in all four chambers.

I. COMPRESSOR ROOM (Room 71)

****WARNING****

Approved hearing and eye safety protection must be worn at all times in the RSF's compressor room. Compressor air control lines are pressurized at all times, even with the RSF compressors not operating.

1. Notify (b) (6) the demand being placed on the process cooling water system prior to starting the compressor(s). Normal process cooling water system pressure is 35 to 75 PSI.

2. Ensure large red handled shop air supply valve in the compressor room is closed.

3. Inspect the compressor air receiver automatic condensate drain line for damage and that the automatic drain is operating.

4. Verify the exhaust louvers are open.

5. Verify the RSF air dryer ball valves are in the proper configuration. Refer to the drawing on the wall, or in the RSF Operators Guide. During normal operation when the PSEF shop air compressors are working properly, valves will be configured so that the RSF air compressor control air is supplied by the PSEF shop air compressors.

6. Utilize the Centac Compressor Checklist (located on the front of each compressor) to start the desired RSF compressor.

7. Verify compressor output is set to 125 psi, and that compressor is operating properly.

II. TEST CHAMBER AREA HOOKUP AND PRESTART

Section II of this checklist is accomplished after the test chamber lid, with the test article installed, is properly installed on the test chamber and all lines are connected

****WARNING****

Approved hearing and eye safety protection must be worn at all times in the RSF's test cell rooms and shop area.

Ensure that the drive turbine's compressed air supply line, manual ball valve (Yellow handle located near the proportional valve), and the condensate drain valve (located on the air pressure regulator), both remain closed when working around the test chamber or connecting/disconnecting the drive turbine drive or brake lines!

****CAUTION****

All hoses utilizing quick disconnects (QD) must be checked for positive engagement before pressurizing. This is accomplished by physically tugging on the hoses after connecting them.

1. Check the oil scavenge hose for positive QD engagement.

2. Check drive turbine bearing oil supply for positive QD engagement.

3. Check the damper oil supply hose for positive QD engagement.

4. Check all electrical connections for proper connection.

5. Verify the drive and brake air lines are properly connected and tight.

6. Verify the drive and brake air pressure indicator lines are properly connected and tight.

7. Verify the speed probe cannon plugs are properly connected and secure.

8. Verify the proximity probe cables are properly connected and secure.

9. Verify all thermocouple leads are properly connected and secure.

10. Verify that the heat exchanger cooling water valves are open for the heat exchanger on the drive turbine oil cart.

11. Verify that the drive turbine oil cart is plugged into the red wall receptacle and that the back-up compressed air line is connected.

12. Turn on the oil cart and verify flow in the oil flow gauges. Verify that bearing and damper oil pressures are both adjusted to 20psi.

13. Verify there are no oil leaks.

14. Close the spin pit vent valve.

15. Verify the valves for the vacuum pump pcw valves are open.

16. Utilize the vacuum pump checklist to start vacuum pump(s).

17. Start the RSF cooling loop in room 84. The specific start-up instructions are posted in room 84.

18. Ensure the proper entries are made in the Vacuum Pump logbook in the control room.

19. Open the PSEF shop air valve (located on top of the spin chamber on the wall).

20. Verify the balance air pressure is adjusted to value specified in the test plan.

21. If the vacuum pumps are properly warmed up, open the vacuum pump isolation valves and begin pulling vacuum.

III. CONTROL ROOM PRESTART:

1. Verify that the three toggle switches for the Main Air, Brake air, and Drive Air are still in the "Off" position.

2. Verify that the Pacific is configured for 6 tooth speed nut input. (first day of testing only).

3. Verify that the large tachometer is set to the proper overspeed alarm set point per the test plan.

4. Turn on the OpData computer and open the Pacific software. Click on "Display Definition" and open the operators screen. Click on Acquisition. Click on preview. Verify that Pacific Data is reading properly.

5. Power on the BSI computer and open the Spin IV software.

6. Click on "configuration" and select "test parameters" from the drop down menu. Verify limits are correct based on the test plan. **NOTE** If you have to change any values, you must hit enter after each

value you change in order to save the change. When all parameters are correct, click on the "Download Edits" button.

7. Utilize the "configuration" drop down menu to select the "valve offsets" window.

8. Utilize the "status" drop down menu to open the "general status" window.

9. Utilize the "testing" drop down menu and open the "manual testing" window.

IV. FINAL TEST CELL CLOSE UP

1. In the test cell, open the large yellow main air supply valve.

2. In the test cell, double check all oil and water lines to ensure no leaks.

3. Clear the chamber of all personnel

4. Close and secure all test cell doors. Ensure outside doors are locked

5. Verify the "Test in Progress" light and the equipment in use lights are on for spin pit #1 and the compressor room. Visually verify all lights are operational.

6. Verify that the Astromed recorder is open to the correct file and that the green arrow is illuminated indicating strip chart operation.

7. Increment the Pacific Single Scan file and begin recording.

8. You are now set up and ready to test. Follow the procedures in the HCF operators guide and the test plan for specific instructions related to this test. Utilize this checklist for test shutdown and cell close-up at the completion of testing.

V. END OF DAY SHUTDOWN AND CELL SECURITY

1. Verify that test article RPM has reached "0" and place all three air control toggle switches in the "Off" position.

2. Stop the Astromed recorder and the Pacific Single Scan.

3. In the spin chamber, inspect the top of the spin lid for any signs of leaks or damage.

4. Close the PSEF Shop air valve to secure balance air.

5. Close yellow main air valve.

6. Close the vacuum pump isolation valves, and follow the vacuum pump checklist to turn off the vacuum pump(s).

7. Open the 2" ball valve to vent the spin chamber.

8. Turn off the cooling system in room 84.

9. Utilize the Centac checklist to turn off the RSF air compressors.

10. Secure the Drive Turbine Oil Cart and unplug the electric plug.

11. If testing is scheduled to continue the next day, it is not necessary to close any further valves.

12. Follow the instructions provided for disconnected and removing spin pit lid.

13. Turn off the "Test-In-Progress" and "Equipment-In-Use" lights.

Appendix D (Emergency Procedures)

The following procedures shall be followed for the emergency scenarios detailed below:

Scenario # 1: **Loss of speed control: Due to a problem with instrumentation or control hardware, the test article no longer responds to control inputs or safety limits.**

- **Stop Test**
  - Test Abort: Hit abort in the Spin IV software or the red abort button on the TC-4 twice to bring the speed to zero rpm.
  - Manual Mode: Centering the three speed control toggle switches will cut off air from the drive and brake lines. Toggling the main air and brake air switches to "Manual" will allow for a manually controlled deceleration to a stop.
  - Emergency Stop Button: If the other methods fail to stop the test article, the red E-Stop button on the control panel will prevent the rotor from continuing to accelerate (coast mode).
- **Troubleshoot Control Problem**

Scenario # 2: **Loss of Speed Indication: Due to an instrumentation problem, there are either no speed indications or the indications are different between the two probes.**

- **Stop Test**
  - Test Stop: Hit abort in the Spin IV software or the red abort button on the TC-4 to bring the speed to zero rpm.
  - Manual Mode: Centering the three speed control toggle switches will cut off air from the drive and brake lines. Toggling the main air and brake air switches to "Manual" will allow for a manually controlled deceleration to a stop.
  - Emergency Stop Button: If the other methods fail to stop the test article, the red E-Stop button on the control panel will prevent the rotor from continuing to accelerate (coast mode).
- **Troubleshoot Control Problem**

February 2017
Volume 86

Naval Aviation Enterprise S&T SitSum

NAE Chief Technology Office (CTO) *NAVAIR 4.0T*

Welcome to the NAE S&T SitSum

The Naval Aviation Enterprise (NAE) Science & Technology (S&T) Situational Summary (SitSum) is a succinct overview of items of potential interest to Senior Leadership via email. Requests to be added to the distribution should be sent to: naecto@navy.mil

To learn more, please visit the NAE CTO SharePoint site at: https://myteam.navair.navy.mil/air/40/40t/default.aspx

In This Edition:

In its 17th year, the Department of the Navy's "Forum for SBIR/STTR Transition" (FST) - the small business technology exposition – will take place on April 3rd through 5th 2017, at the Gaylord National Harbor , MD in collaboration with the Navy League's Sea-Air-Space Exposition.

The purpose of joining the forums is to bring small businesses, system integrators, and large contractors together to establish a dialogue that will hopefully yield technologies never before envisioned or affordable.

This collaboration marries large and small business marketplaces for defense technology together with our respective requirements / needs as the focal point. The events have attracted top Congressional leaders and senior Navy leadership. The expectation is that significant commercialization possibilities may result from this alignment and to increase the ability to deliver innovation quickly to the warfighter.

S&T Dates of Interest

MARCH

6TH - 10TH
2017 Pacific Operational S&T Conference
Hilton Hawaii Village
Honolulu, HI
http://www.ndia.org/meetings/7540/Pages/default.aspx

6TH - 8th
32nd Annual Test & Evaluation Conference
San Diego Marriott Mission Valley
San Diego, CA
http://www.ndia.org/meetings/7910/Pages/default.aspx

7th - 8th
2017 Human Systems Conference
Waterford at Springfield
Springfield, VA
http://www.ndia.org/meetings/7350/Pages/default.aspx

22nd - 23rd h
Ground Robotics Capabilities Conference & Exhibition
Waterford at Springfield
Springfield, VA
http://www.ndia.org/events/2017/3/22/ground-robotics-capabilities

The SBIR/STTR Transition Forum has evolved to become the intersection of DON acquisition needs and SBIR/STTR solutions. The success metric from the first Forum in 2000 was the investment in, or purchase of SBIR/STTR technologies averaging $1.2 million within 18 months for more than half of the Forum participants.

More than 100 SBIR/STTR companies will be exhibiting rapidly maturing Phase II technologies at the Forum. An improved acquisition-focused curriculum in the technical assistance program for DON SBIR/STTR contractor's industry outreach helps to underpin larger defense firms to install a strong business model / rational for the inclusion of SBIR/STTR engagement

The Forum's Small Business Exhibition will feature focused SBIR/STTR technologies with more than 100 exhibits in a hall adjacent to S-A-S, open throughout the S-A-S event. Both large and small businesses, as well as Naval acquisition personnel, will have the opportunity to conduct one-on-one meetings with participating SBIR/STTR contractors. As always, the Forum will host an impressive list of keynote speakers.

Registration for the forum is free and includes entrance to the S-A-S exhibit and all S-A-S free events. S-A-S attendees also have free access to the SBIR/STTR forum, including the presentations and small business technology exhibits.

Highlights from the 2016 DoN FST can be viewed here.

Over 100 participating small businesses are showcased in the Virtual Transition Marketplace (VTM). Search for technologies, or sort by SYSCOM. The VTM is the place to learn more about the companies. In a Quad Chart format a brief description of the technology, the SBIR company and how this technology will benefit the Navy and transition to the fleet. Contact information on each company, along with a capability brochure, is provided for review. See something you like? Users can also create a personalized "Briefcase" and add the company for future consideration and follow up buy printing a copy, e-mail or even view the briefcase on their mobile device at the Forum. To meet the companies that interest you, sign up for a 1-on-1 meeting with these small businesses here.

Registration for the FST Forum for the 2017 is now open:

https://events.sa-meetings.com/ereg/index.php?eventid=215155&

For additional information, contact: stpinfo@atsicorp.com.

S&T Dates of Interest, con't

27th - 29th
Munitions Executive Summit
Hilton Parsippany
Parsippany, NJ
http://www.ndia.org/events/2017/3/27/munitions-executive-summit

28th - 29th
Precision Strike Annual Review
Waterford Conference Center
Springfield, VA
http://www.precisionstrike.org/Events/7PPR/7PPR.html

APRIL

3rd - 5th
Sea-Air-Space: The Navy League's Global Maritime Exposition
Gaylord National Resort & Convention Center
National Harbor, MD
http://www.seaairspace.org/

3rd - 5th
2017 DoN FST (Forum for SBIR/STTR Transition)
Gaylord National Resort & Convention Center
National Harbor, MD
https://navyfst.com/

18th - 20th
18th Annual Science & Engineering Technology Conference
National Defense University
Washington, DC
http://www.ndia.org/events/2017/4/18/7720

19th - 20th
33rd Annual National Logistics Forum
Tampa Airport Marriott
Tampa, FL
http://www.ndia.org/meetings/7730/Pages/default.aspx

24th - 26th
2017 Joint Undersea Warfare Technology Spring Conference
Admiral Kidd Conference Center
San Diego, California
http://www.ndia.org/events/2017/4/24/7260

25th - 26th
2017 Mission Engineering workshop
University of Mary Washington, Dahlgren Campus
Dahlgren, VA
http://www.navalengineers.org/Events/Event-Info/sessionaltcd/MISSIONENG2017

Harvey leads award-winning team to SERDP Project-of-the-Year

By (b)(6),

NAWCWD Public Affairs Office

In 2012, (b)(6) and his team at the Naval Air Warfare Center Weapons Division, along with collaborators from the Air Force Research Laboratory at Edwards Air Force Base and the Naval Research Laboratory, were awarded a 4-year grant from the Strategic Environmental Research and Development Program to develop high temperature polymers and polymer composites derived from renewable sources.

Their project titled, "Cyanate Ester Composite Resins Derived from Renewable Polyphenol Sources," was highly successful and, on December 6, 2016, the team was honored with SERDP's 2016 Project-of-the-Year Award for Weapons Systems and Platforms.

Dr. Harvey stated that he was very pleased and excited when he found out that this award was the direct result of the hard work and dedication of all the team members. We've had the opportunity to publish and patent a lot of paradigm-changing work in this field, but none of it would have been possible without my colleagues, the support of management, and the opportunity afforded by SERDP."

Composite materials made by combining a thermosetting resin with a rigid structural component such as carbon fiber are widely used by the Department of Defense in place of metal or ceramic materials due to their ability to reduce weight and fuel usage. In many cases, these composites are stronger, more durable and less susceptible to corrosion than engineered metals leading to longer life-cycles and decreased maintenance costs.

The issue, Dr. Harvey explained, is that thermosetting resins are currently derived from petroleum resources by unsustainable, energy intensive, multistep methods that utilize substantial amounts of organic solvents. To combat this, he and his project team have been working to utilize a bio-synthetic approach based on molecules like vanillin, the main component of vanilla extract, which can be produced from wood, and resveratrol, an antioxidant present in grape skins, red wine and blueberries. These natural compounds can then be converted to thermosetting resins like cyanate esters through efficient, high throughput chemistry.

Most people assume that bio-derived materials exhibit reduced performance compared to conventional, petroleum-derived materials. In contrast, this program has shown that 'bio-derived' and 'high performance' are not mutually exclusive terms. Several of the resins developed in this project outperform conventional resins derived from petroleum.

For example, the team has made a virtually flame-proof resin from resveratrol that has a glass transition temperature greater than 350 degrees celsius. Small-scale testing of this material by the Federal Aviation Administration showed that it had one of the lowest heats of combustion of any polymer they've studied. They've also developed a polymer derived from pine resin that can be placed in boiling water for four days without any degradation or change in its thermomechanical properties.

According to Harvey, several of the polyphenols synthesized by NAWCWD have no estrogenic effects unlike petroleum derived resins made from Bisphenol A (BPA) and the bio-synthetic approach has the potential to offer a virtually unlimited supply of sustainable, low toxicity, bio-based polyphenols and resins for both DoD and commercial use.

Beyond the small-scale synthesis of new bio-derived molecules, Harvey and his team have fabricated and tested flat panels made with carbon fiber, glass or quartz impregnated with the resins. They have also developed new bulk molding compounds that can be fabricated into virtually any shape. Using this approach, the team has successfully fabricated a part that acts as a connector for a nozzle and missile case.

Harvey wasn't always interested in polymer chemistry.

"I'm a classically trained inorganic/organometallic chemist and spent most of my time in graduate school synthesizing esoteric transition metal compounds," Harvey said. "When I started working at NAWCWD as a postdoctoral fellow in 2006, I never thought I'd be working with bio-based polymers, but our mission is to support the warfighter and this work has the potential to make a real impact."

The SERDP yearly award recognizes scientific advances and technological solutions to some of DoD's most significant environmental challenges and looks for projects that will help DoD enhance its mission capabilities, improve its environmental and energy performance, and reduce costs. For more details on Harvey's project, visit SERDP's site at https://serdp-estcp.org/News-and-Events/Blog/Cyanate-Ester-Composite-Resins-Derived-from-Renewable-Polyphenol-Sources

(b)(6), right, celebrates with his (b)(6) n teammates on Jan. 12 at China Lake after winning the Strategic Environmental Research and Development Program 2016 Project-of-the-Year Award. From left to right are Dr (b)(6)

DoD Science, Technology, and Innovation Exchange – Call for Abstracts

Office for Basic Research
Office of the Assistant Secretary of Defense for Research and Engineering
Department of Defense

The Basic Research Office is proud to announce the roll-out of a platform that will enable members of the Defense Science &Technology (S&T) community to share ideas surrounding DoD-sponsored science with each other and with broad

audiences. The Science, Technology, and Innovation exchange – STIx – is the first event of its kind. STIx will showcase the extensive S&T investments, outcomes, and innovations from across the Defense enterprise, including industry and academia. STIx takes its cues from TED and TEDx series of talks and seeks to showcase and connect our brightest minds, to communicate new ideas and share novel approaches to confronting old challenges facing the Defense community.

The inaugural STIx event will be held in Crystal City, Virginia from June 22nd -23rd 2017. The event will consist of a series of presentations based on the theme of "The Big Question." We invite submission of abstracts for STIx to address the meeting's theme. Specifically, abstracts for these presentations should address one of more of the three major subtopics:

I. The big question that my research seeks to answer
II. The big question that my technology addresses
III. The big question of identifying, nurturing, recruiting, and/or retaining top STEM talent to ensure the nation's present and future intellectual capacity and security

Targeted speakers for the event include:

- Scientists from colleges/universities and DoD laboratories
- Student participants in the Science, Mathematics, and Research for Transformation (SMART) Scholarship Program, and the National Defense Science & Engineering Graduate Fellowship (NDSEG)
- K-12 science teachers that have participated in DoD sponsored programs

We welcome submissions for a carefully prepared talk or demonstration that reports issues, ideas, or findings related to basic science, multidisciplinary and/or cross-organizational work, technological advances, or best practices related to STEM education. Please keep in mind that all presentations must be distribution A, communicable to a broad audience.

Please send abstracts to (b)(6) by 28 April 2017 at NOON. We will send prospective speakers formal invitations via email not later than 12 May 2017.

STIx event registration information will follow in a separate notice.

The High Frequency Gravitational Wave Generator

(b)(6), NAVAIR/NAWCAD

Aerospace Engineer AIR 4.4.5.1

This inventive concept proposes that it may be possible to generate high-power / high-frequency gravitational waves (HFGWs) by high-frequency, accelerated, axial rotation (spin) and / or accelerated, high-frequency vibration of an electrically charged, asymmetric structure. This phenomenon is highly non-linear in nature but is possible within the context of non-equilibrium thermodynamics, which significantly differs from equilibrium physics. In February of 2016 the National Science Foundation publicly announced that the Laser Interferometry Gravitational Wave Observatory (LIGO) had after much experimentation detected gravitational waves emanating from the collision of two stellar mass black holes, thereby showing the physical reality of such waves which further supported General Relativity (GR) theory predictions.

Think of the gravitational waves as "ripples" or undulations in the curvature of the space time continuum. These ripples propagate fluctuations in gravitational fields which arise due to the dynamics of massive physical entities whose motion is represented by high-frequency / high-energy, highly non equilibrium dynamics.

The asymmetric structure of the High Frequency Gravitational Wave (HFGW) Generator has the ability to control the accelerated modes of vibration and to spin off its electrically charged surfaces, in particular the rapid rate or change of the cyclic nature of accelerated-decelerated-accelerated vibration and gyration (axial spin) of these electrified surfaces. In this manner the onset of relaxation to thermodynamic equilibrium is delayed which generates a physical mechanism that may induce anomalous effects. For instance under certain conditions which involve rapid acceleration transients, one can mathematically demonstrate an exponential growth in the fields and electromagnetic energy flux with accelerating vibration. In the present concept the high-power HFGWs are generated by enabling the Gertsenshtein effect (see Figure 1), i.e., producing a gravitational wave by propagating electromagnetic radiation through strong magnetic fields.

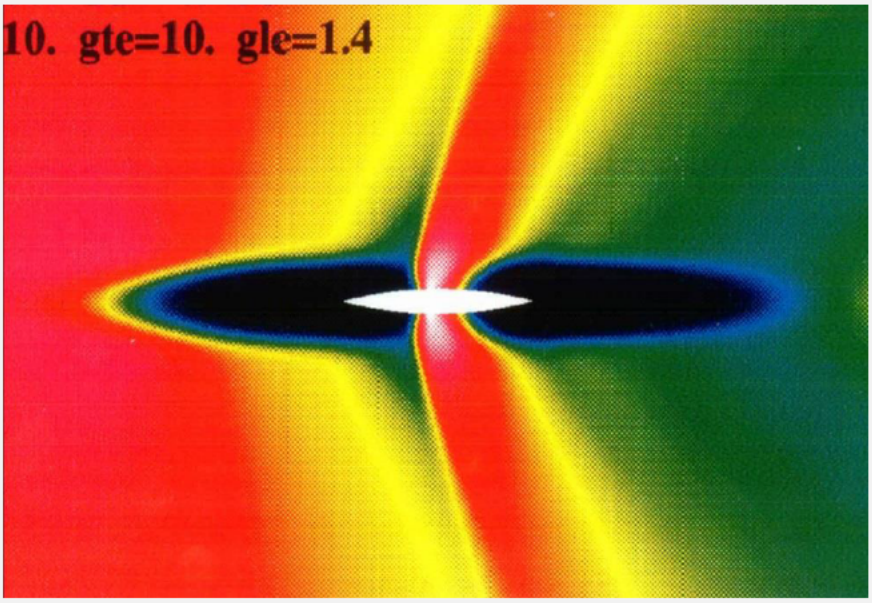

Figure 1: Formation of a flight-assisting, zero-point radiation pressure gradient about an accelerating craft that is emitting and depositing Electromagnetic Field energy into the craft's surrounding Quantum Vacuum [From CFD simulation by Robert L. Roach]. Shown with permission from Herman David Froning (copyright 2017)

Controlled motion of charged matter under rapid-acceleration transients may enable macroscopic quantum coherence and therefore quantum mechanical behavior of macroscopic objects. Moreover, the accelerated vibration and / or spin of the charged matter may generate high–power, high frequency gravitational waves which can be used in a variety of applications, such as advanced field propulsion e.g., the design of a workable space drive. Therefore, it may be possible to propel a spacecraft equipped with a HFGW generator by producing high-frequency gravitational waves, which in turn would generate their own gravitational fields upon which the craft would propagate in a wave-surfing fashion.

"High Frequency Gravitational Wave Generator" Navy case PAX 233 was filed with the United States Patent & Trademark Office Serial # 15431823 on February 14th, 2017. An interesting aspect of this patent application is that it couples the generation of high frequency gravitational waves (HFGWs) with the possibility of room temperature superconductivity (RTSC). Both of these apparently disparate concepts would be related to the far-from-equilibrium dynamics of electrically charged matter. If possible by controlling the motion of charged matter under the non-equilibrium condition of rapid acceleration transients, numerous advancements in Science and Technology (S&T) become possible such as an advanced arguably Emergent Physical Phenomenon.

If possible the achievement of room-temperature superconductivity (RTSC) represents a highly disruptive technology, a total paradigm shift with potentially enormous military and commercial applications. Furthermore the internal heating by any system enclosure can be greatly reduced by RTSC wiring, which would allow complete transmission of electrical power to its subsystems.

Temperature, current density, and externally-applied, magnetic-field strength are the three main parameters which affect superconductivity. Physically, these parameters have one thing in common, the motion of electric charges (i.e., electrons). Control of this motion via vibration and / or spin of charged matter subjected to rapid acceleration transients (highly non-linear in nature) may lead to the achievement of RTSC, especially if the charged matter is non homogeneous.

The key to RTSC may be to enable local, macroscopic, quantum coherence, namely the ability of a macroscopic object to act as if quantum mechanical in nature exhibiting such phenomena as superposition, entanglement, and tunneling. If all you need to do in order to make a special composite metal wire superconductive (SC) at room temperature is to abruptly vibrate it (which may or may not be mechanically induced) while running a time independent current through it would enable possible applications which are extremely significant.

The answer to this question can only come from experimental verification of the concept in the laboratory, the success of which can bring about a total paradigm change in S&T. Currently (b)(6) is funded to prove / validate the theory that high energy electromagnetic field intensities can be generated under laboratory conditions, which if successful will introduce a complete, seemingly unbounded paradigm shift, and possibly validate the concept at hand

ESTCP Solicitation for FY 2018 Funding: INSTALLATION ENERGY AND WATER TECHNOLOGIES

JUST RELEASED! ESTCP FY 2018 SOLICITATION

The Department of Defense's (DoD) Environmental Security Technology Certification Program (ESTCP) released a solicitation on February 2, 2017, requesting proposals for demonstrations of installation energy and water technologies.

BROAD AGENCY ANNOUNCEMENT (BAA): The BAA requests pre-proposals related to:

- Innovative Technology Transfer Approaches
- Innovative Approaches to Obtaining Authority to Operate for Facility-Related Control Systems
- Energy Efficiency Technology Demonstrations Integrated with Utility Energy Service Contracts (UESC)

DOD and FEDERAL ORGANIZATIONS OUTSIDE DOD: The DoD Call for Proposals and Call for Proposals for Federal Organizations Outside DoD request pre-proposals responding to the following topics only:

- Innovative Technology Transfer Approaches
- Innovative Approaches to Obtaining Authority to Operate for Facility-Related Control Systems

The due date for all pre-proposals is April 6, 2017 by 2:00 p.m. ET. More information about the solicitation, including instructions and deadlines, is available on the ESTCP website under Funding Opportunities (https://serdp-estcp.org/Funding-Opportunities/ESTCP-Solicitations/Installation-Energy-Solicitation).

NAE S&T Metrics

The NAE CTO tracks and regularly updates the NAE S&T Metrics. This edition of the SitSum highlights the NAE FY15 S&T investment portfolio aligned to the eleven capability gaps identified in the 2014 NAE S&T Objectives document.

The NAE S&T FY15 Portfolio had 825 projects, with a total investment of $402.8M.

For FY15, the largest share of the S&T investment addressed issues in the Information Dominance (ID) area, followed by Enterprise and Platform Enablers (EPE).

Capability Gap	# of Projects	Total FY15 Funding	% of Total FY15 Investment
Enterprise and Platform Enablers (EPE)	246	$69.0M	17%
Force Protection (FP)	38	$25.7M	6%
Information Dominance (ID)	125	$80.6M	19%
Integrated Logistics Support (ILS)	24	$16.3M	4%
Naval Warrior Performance (NWP)	77	$24.5M	6%
Non-Naval Aviation	1	$0.1M	1%
Strike Operations (STK)	53	$30.0M	7%
Surface Warfare (SUW)	28	$30.4M	8%
System Safety, Availability and Affordability Enablers (SSAA)	141	$47.9M	12%
Theater Air and Missile Defense (TAMD)	18	$26.1M	7%
Under Sea Warfare (USW)	74	$52.2M	13%
Total:	**825**	**$402.8M**	**100%**

Activity 1-3 investment, plus SBIR/STTR, Transition Funding, ex: Rapid Innovation Fund / TIPS, and Congressional Adds
** Programs and projects are not the same; S&T "programs" can generate multiple "projects"
*** SBIR totals includes STTR investment and PEO (Carriers) SBIR funding

Data Source: NAE S&T Alignment & Reporting System (STAIRS) Oct 20 2016

S&T Program Calendar: MARCH

Upcoming S&T events, calls for proposals, S&T briefings and conferences for March 2017 are shown below:

Day	Event
1	FY17 Rapid Innovation Fund: OSD releases FY17 BAA (End of open comms with vendors, comms on Focus Area (FA) reqt permitted between vendor and FA TPOC)
2	FY18 Section 219 Proposals due to the CTO from the T-Codes
2 - 3	FY18 Foreign Comparative Testing (FCT): Navy Draft Review Board
3	SBIR 18.1 and 18.A: Topics due to SBIR office via STAIRS
12	Coalition Warfare Program (CWP) Presentations at Pentagon
14	S&T IPT Meeting
23	FY18 Section 219 WFD: Thrust Area Champion Reviews Due to CTO
24	SBIR PMA 18.1 endorsements and 18A interest statements due
25	FNC POM 20 Gaps due to OPNAV N941
27	FY18 Section 219 Basic and Applied Research (BAR) and Transition call for proposals issued by CTO
28	S&T IPT Meeting

The High Energy Electromagnetic Field Generator (HEEMFG) (219BAR-17-009)

(b)(6), Air 4.3.5.1, (b)(6)@navy.mil, Project Type: (BR)

Overview

- **OBJECTIVE** | Design a test article and instrumentation to demonstrate the experimental feasibility of achieving high electromagnetic (EM) field-energy flux values toward the design of Advanced High Energy Density / High Power Propulsion Systems.
- **THE NEED** | Advanced High Energy Density / High Power Propulsion Systems are needed to counteract Adversary Capability Surprises and Hybrid Warfare Tactics.
- **POTENTIAL USE CASE/MILITARY APPLICATIONS** | Realization of this technology moves propulsion technology beyond gas dynamic systems.
- **NDS ALIGNMENT**
  - Space and cyberspace as warfighting domains
  - Missile Defense
  - Evolve innovative operational concepts

FY18 Activity/Accomplishments

- **"High Frequency Gravitational Waves - Induced Propulsion"** published as peer-reviewed SAE Technical paper 2017-01-2040 , October 03, 2017. Presented at the SAE AeroTech Congress & Exhibition.
- - It may be possible to generate high power / high frequency gravitational waves (HFGWs) by high frequency accelerated axial rotation (spin) and/or accelerated high frequency vibration of an electrically charged, possibly asymmetric structure, within the context of non-equilibrium thermodynamics, namely far-from-equilibrium physics, highly non-linear in nature. Therefore, it may be feasible to propel a hybrid craft equipped with an HFGWG, by producing high frequency gravitational waves which in turn generate their own gravitational fields upon which the craft would propagate in a 'wave-surfing' fashion.
- **Navy Case PAX 285 titled "Plasma Compression Fusion Device"** has been filed with the United States Patent & Trademark Office as a patent application / Serial # 15928703, on March 22, 2018.
- - The Plasma Compression Fusion Device (PCFD) generates energy gain by plasma compression-induced nuclear fusion, via a novel method of magnetic confinement. This concept has the capability of maximizing the product of plasma pressure and energy confinement time in order to maximize energy gain and thus give rise to fusion ignition conditions. Moreover, this invention can give our Navy the technological edge in achieving National Energy Dominance, besides its many commercial benefits in energy generation.

Project Overview

Technical Approach: $S_{max} \approx (Q^2 / \varepsilon_0)\ (R_v^2 / R_s^5)\ \Omega\ [\exp(2\,\Omega\, t)]$

- By coupling an electrically charged system's high frequency of axial spin (with accelerated vibration), operated in a rapidly accelerated transient mode, this project could achieve extremely high electromagnetic field-intensity (EM energy flux) values.
- This experimental investigation has several tasks, namely to design the experiment, the test asset, the associated instrumentation, the power requirements, and then to perform Spin Test.

NAWCAD Benefit:

- Realization of this HEEMFG technology moves the propulsion and power arena beyond gas dynamic systems and enables the design of a field propulsion-based hybrid aerospace-undersea craft, capable of multi-domain missions. Controlled Motion of electrically charged matter (from solid to plasma) via Accelerated Spin and/or Accelerated Vibration under Rapid Acceleration Transients , can result in high intensity electromagnetic energy flux, thereby resulting in novel energy harvesting and generation techniques and devices. These devices can greatly enhance NAVAIR/NAWCAD's electronic warfare technologies arsenal. Moreover, this work can result in the enablement of **Macroscopic Quantum Coherence**, that is the engineering of macroscopic states to behave as if quantum mechanical in nature - this is revolutionary for the Emerging field of Quantum Technologies, with applications in Quantum Computing, Spintronics, Artificial Intelligence, Crypto., etc.
- Furthermore, this technology has National Security importance in leading to the generation of thermonuclear Fusion Ignition Energy with commercial as well as military application potential, in ensuring National Energy Dominance.

Accomplishments:

- Completed preliminary experiments / test asset charging / EM flux detector mfg.
- Will complete test asset design and perform Spin Test to detect HEEMFG effect.

COIN CELL CAPACITOR SPIN RIG

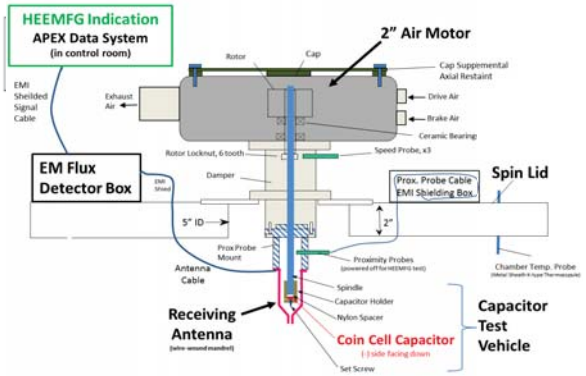

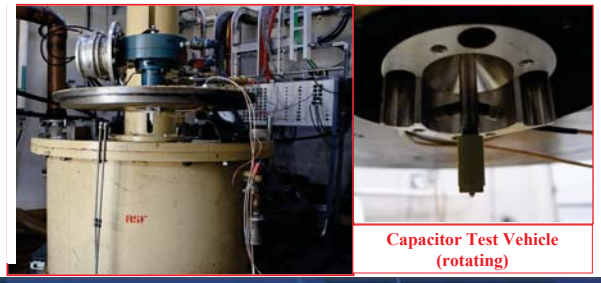

Capacitor Test Vehicle (rotating)

Transitions/Future

- The HEEMFG work can lead to the development of Advanced Power Systems which can be used to enhance Distributed Maritime Operations.
- Naval Electronic Warfare, Advanced Hypersonic Systems, Quantum Technologies, and Advanced Power Generation Systems would also greatly benefit from HEEMFG experimental results.
- Results of the HEEMFG experimental study can lead to future collaborations with ONR, NRL, and/or DARPA. At present HEEMFG experiments use spin configurations only, in the future, accelerated vibration coupling is envisioned.

Collaboration/Workforce Development/Bibliometrics

- **The HEEMFG experimental study is a highly collaborative NAWCAD / AIR 4.4 and AIR 4.3 effort.**
  - –Currently working with (b)(6) (Co-PI), (b)(6) and (b)(6) on test asset design and test directive preparation.
  - –Working with (b)(6) and HEEMFG Team on the EM Flux Detector design and testing.
- **Technical paper AIAA 2019 0869, titled "Room Temperature Superconducting System for use on a Hybrid Aerospace-Undersea Craft"** was successfully presented at the 2019 AIAA SCITECH Forum and Exposition (Jan.07-11) in San Diego, CA. This breakthrough paper presents a strong theoretical concept for achieving room temperature superconductivity (RTSC) in a current-carrying special composite metal wire. This concept enables the transmission of electrical power without any losses, which leads to the design and development of novel energy generation and harvesting devices with important benefits to civilization.